

The quantum detection of projectors in finite-dimensional algebras and holography

Joseph Ben Geloun^{a,c,*} and Sanjaye Ramgoolam^{b,d,†}

^a*Laboratoire d'Informatique de Paris Nord UMR CNRS 7030
Université Paris 13, 99, avenue J.-B. Clement, 93430 Villetaneuse, France*

^b*School of Physics and Astronomy, Centre for Research in String Theory
Queen Mary University of London, London E1 4NS, United Kingdom*

^c*International Chair in Mathematical Physics and Applications
ICMPA–UNESCO Chair, 072 B.P. 50 Cotonou, Benin*

^d*School of Physics and Mandelstam Institute for Theoretical Physics,
University of Witwatersrand, Wits, 2050, South Africa*

E-mails: *bengeloun@lipn.univ-paris13.fr, †s.ramgoolam@qmul.ac.uk

Abstract

We define the computational task of detecting projectors in finite dimensional associative algebras with a combinatorial basis, labelled by representation theory data, using combinatorial central elements in the algebra. In the first example, the projectors belong to the centre of a symmetric group algebra and are labelled by Young diagrams with a fixed number of boxes n . We describe a quantum algorithm for the task based on quantum phase estimation (QPE) and obtain estimates of the complexity as a function of n . We compare to a classical algorithm related to the projector identification problem by the AdS/CFT correspondence. This gives a concrete proof of concept for classical/quantum comparisons of the complexity of a detection task, based in holographic correspondences. A second example involves projectors labelled by triples of Young diagrams, all having n boxes, with non-vanishing Kronecker coefficient. The task takes as input the projector, and consists of identifying the triple of Young diagrams. In both of the above cases the standard QPE complexities are polynomial in n . A third example of quantum projector detection involves projectors labelled by a triple of Young diagrams, with m , n and $m+n$ boxes respectively, such that the associated Littlewood-Richardson coefficient is non-zero. The projector detection task is to identify the triple of Young diagrams associated with the projector which is given as input. This is motivated by a two-matrix model, related via the AdS/CFT correspondence, to systems of strings attached to giant gravitons. The QPE complexity in this case is polynomial in m and n .

Key words: quantum information, complexity, ads/cft, tensor models, Kronecker coefficients.

Contents

1	Introduction and Outlook	2
2	Background	6
2.1	The group algebra $\mathbb{C}(S_n)$ and its centre $\mathcal{Z}(\mathbb{C}(S_n))$	6
2.1.1	A heuristic argument for the asymptotics of $k_*(n)$ at large n	8
2.1.2	$k_*(n)$, Casimirs of $U(N)$ and multipole moments	8
2.1.3	Unitary operators	9
2.2	Quantum Phase Estimation	10
3	Quantum Phase Estimation for projectors in the centre of $\mathbb{C}(S_n)$	14
3.1	QPE for T_2	15
3.2	General procedure for arbitrary n	15
3.2.1	Dimension of the register space for eigenvalues of general T_k	16
3.2.2	Query and gate complexities at general n	17
4	Classical algorithm related to quantum projector identification by holographic duality	18
5	Classical matrix algorithms for projector detection: randomised classical algorithm	23
5.1	Discussion and future directions	28
5.1.1	Interpretation	28
5.1.2	One dimensional representations	29
5.1.3	More general choices of V	29
6	Detection of the Kronecker projector in $\mathcal{K}(n)$	29
7	Detection of the Littlewood-Richardson projector	34
A	Representation theory lemmas used in quantum-inspired classical algorithms	36
B	Solving the power sums M_k	37
C	Proof of a property of Kronecker projectors	38

1 Introduction and Outlook

With motivations from the holographic AdS/CFT correspondence [1, 2, 3] and other gauge-string dualities (e.g. [4, 5]), we consider the quantum computational task of de-

tecting projectors in finite dimensional associative algebras. These algebras we consider are semi-simple and have a Wedderburn-Artin (WA) decomposition as a direct sum of matrix algebras (see a general exposition of the WA decomposition in, e.g. [6]). They are related to symmetric groups S_n of all permutations of n objects. The WA decompositions can be constructed using representation theory data from symmetric groups, such as characters of irreducible representations (irreps), matrix elements of permutations in these irreps and branching or Clebsch-Gordan coefficients. The projectors of interest act as the identity in a fixed matrix block of the WA decomposition and zero elsewhere. They are thus labelled by the representation theory data specifying the matrix blocks. Given their relation to symmetric groups, the algebras also have combinatorial bases related to equivalence classes of permutations. These combinatorial bases are used to construct central elements in the algebras of interest. They are exponentiated to give unitary operators in Hilbert spaces formed by the algebras themselves. Our detection task proceeds with the standard technique of quantum phase estimation (QPE) [7], using these unitary operators as quantum gates which are applied to query the projectors. The set-up is usefully viewed in the context of a quantum communication between Bob, who builds the projector and sends it to Alice, who identifies the projector using QPE. Combining results on query complexities from quantum information theory and facts from the representation theory of S_n , we arrive at complexity estimates which are bounded by polynomials in n .

The AdS/CFT correspondence gives a conjectured equivalence between string theoretic quantum gravity in $AdS_5 \times S^5$ space-time and the non-gravitational quantum theory of $\mathcal{N} = 4$ SYM theory in four dimensions with $U(N)$ gauge group. There are numerous successful tests of the correspondence for interactions of perturbative gravitons (see [8] and the review [9]). Further interesting tests of AdS/CFT involve the quantum states associated with half-BPS giant gravitons [10] and those associated with half-BPS supergravity geometries (LLM geometries) [11]. The labelling of half-BPS CFT operators using Young diagrams and the computation of their correlators [12, 13] plays an important role in the tests involving the interactions of giant graviton branes [14, 15, 16, 17, 18, 19, 20, 21] and the dynamics of strings in LLM geometries [22]. The construction of the CFT operators labelled by Young diagrams and the computation of their correlators for CFT operators of scaling dimension n uses projection operators in the centre of the group algebra $\mathbb{C}(S_n)$ of the symmetric group S_n . The N -dependence of the correlators is controlled by the structure constants of the centre $\mathcal{Z}(\mathbb{C}(S_n))$ of the group algebra $\mathbb{C}(S_n)$ [12]. Recent work [23] has shown that by introducing witness fields in matrix models (matrix couplings in the action or classical unintegrated fields in the observables) the structure constants can be exactly reconstructed.

The correspondence between Young-diagram operators with $n \sim N^2$ and half-BPS bulk geometries motivated the formulation of a toy model of information loss [24]. It was observed that the multi-pole moments of the space-time fields correspond to Casimirs of $U(N)$. It was argued that the ten-dimensional Planck scale bounds the observable

multipoles. This discussion motivated the consideration in [25] of the problem of detecting general Young diagrams with n boxes using a limited number of Casimirs. The problem was formulated, using Schur-Weyl duality, purely in terms of the centre of the symmetric group algebra $\mathbb{C}(S_n)$, denoted $\mathcal{Z}(\mathbb{C}(S_n))$.

The simplest and very interesting Young diagram detection problem in $\mathcal{Z}(\mathbb{C}(S_n))$, inspired by the holographic physics of half-BPS states in $\mathcal{N} = 4$ SYM, is independent of N and concerns the detection of Young diagrams with n boxes. As we explain in section 2, $\mathbb{C}(S_n)$ and $\mathcal{Z}(\mathbb{C}(S_n))$ are Hilbert spaces. It is convenient to use language familiar to quantum information theorists and complexity theorists to describe the detection problem. Bob prepares a quantum state which is a projector P_R in $\mathcal{Z}(\mathbb{C}(S_n))$. He sends the projector P_R to Alice. We will also review the technique of quantum phase estimation for estimating eigenvalues of unitary operators in section 2. Alice applies QPE with a set of unitary operators $\{U_2, U_3, \dots, U_{\Lambda(n)}\}$ to determine the label R of the projector. These unitary operators are exponentials of certain Hermitian operators $\{T_2, T_3, \dots, T_{\Lambda(n)}\}$ which multiplicatively generate $\mathcal{Z}(\mathbb{C}(S_n))$. We will refer to these as cycle central elements. As we explain in section 2.1 choosing the cut-off $\Lambda(n) = n$ suffices to determine R , but we expect that a smaller cut-off will suffice. The cut-off is determined by mathematical properties of $\mathcal{Z}(\mathbb{C}(S_n))$ and is equal to the function $k_*(n)$ identified in [25], as we review in section 2.

The symmetric group S_n acts on n -fold tensor product $V_N^{\otimes n}$ of the fundamental representation of $U(N)$ by permuting the tensor factors. This has been used to construct a basis of half-BPS gauge-invariant operators in $U(N)$ SYM [12] which is orthogonal in the CFT inner product defined by SYM. These Young diagram operators are related by the AdS/CFT holographic dictionary to half-BPS supergravity geometries with $AdS_5 \times S^5$ asymptotics [11]. The symmetric group algebra operators T_k are related to Casimirs in the $U(N)$ theory, by Schur-Weyl duality, and these have in turn been identified [24] with asymptotic charges of the space-time geometries. The problem of quantum detection of projectors P_R labelled by one Young diagram of S_n is thus related by holography to a problem of identifying half-BPS geometries with $AdS_5 \times S^5$ asymptotics from their asymptotic multipole moments. We derive estimates of the complexity of this classical detection in Section 4. It has been recognised that quantum gravity and AdS/CFT present new questions of interest in computational complexity and quantum gravitational physics which can have implications for fundamental questions in computational complexity, such as the extended Church-Turing hypothesis [26, 27]. The half-BPS sector of AdS5/CFT4 and its connection to centres of symmetric group algebras presents a concrete problem of comparison of complexities for a detection task. The estimates we arrive at in section 4 involve $\Lambda(n)$ as well as some intrinsic complexities of gravitational measurements which we leave for future investigation. A more complete treatment of this holographic comparison of complexities should be useful for other instances of holographic CFT-quantum-state/AdS-gravitational-geometry correspondences (see the recent reference for a detailed discussion involving AdS_3 spacetimes e.g. [28]). To get some additional perspective on the

quantum detection of the projectors P_R , we describe a randomized classical algorithm, of the kind used in [29], for the same task in section 5 and give the corresponding complexity estimates.

Section 6 considers the problem of detecting projectors in a Kronecker algebra $\mathcal{K}(n)$ [30, 31, 32] which is a sub-algebra of $\mathbb{C}(S_n) \otimes \mathbb{C}(S_n)$. The algebra is isomorphic to a direct sum of matrix algebras labelled by triples of Young diagrams (R, S, T) with n boxes, where these triples have a non-vanishing Kronecker coefficient $C(R, S, T)$. This is the multiplicity of the trivial representation in the tensor product of S_n irreducible representations $V_R^{S_n} \otimes V_S^{S_n} \otimes V_T^{S_n}$. The matrix algebras have dimension $C(R, S, T)^2$. These algebras control the combinatorics and correlators of invariant observables and correlators of tensor models [31]. We imagine a scenario where Bob constructs the projector and sends it to Alice. Alice can use QPE to identify the triple of Young diagrams in time which is polynomial in n . If the triple (R, S, T) has vanishing Kronecker coefficient, there is no projector for Bob to send to Alice. For this reason the projector detection problem falls short of being a quantum algorithm for determining whether or not a triple of Young diagrams has a non-vanishing Kronecker coefficient. We outline another algorithm, involving communication from Bob to Alice of a simple combinatorial-basis state in $\mathcal{K}(n)$, which has an expansion in projectors associated with all triples (R, S, T) having non-vanishing Kronecker coefficients. Determining whether or not a given triple of Young diagrams appears in this expansion would be a quantum algorithm which determines whether or not the Kronecker coefficient for that triple is zero. We leave the problem of estimating the complexity of this algorithm for future research.

Section 7 concerns a third example of projector detection, based on the algebra $\mathcal{A}(m, n)$ labelled by two integers m, n and defined using equivalence classes of permutations in S_{m+n} modulo conjugation by permutations in $S_m \times S_n$. These algebras arise in the study of 2-matrix invariants relevant to fluctuations of half-BPS giant gravitons in AdS/CFT. The projectors are labelled by a triple of Young diagrams such that the associated Littlewood-Richardson coefficient is non-zero. The algebra was described in [30] along with its decomposition into matrix algebras following earlier work on orthogonal bases for CFT4 correlators in the 2-matrix sector [33][34] [35] [36] [37] [38] [39]. A formulation of a dual classical computation in terms of strings/branes or gravity configurations is an interesting problem for the future.

Additional future research directions are given at the end of most of the sections. Appendix A gives the proofs of two lemmas of quantum inspired classical algorithms used in the main text. Appendix B describes a change of basis in the space of Casimirs of $U(N)$ relevant to section 4. Appendix C proves a property of projectors relevant to section 6.

Note: As this paper was approaching completion, we became aware of [40] and an associated talk at the Perimeter Institute on the ‘‘Quantum Complexity of Kronecker coefficients’’. This has some overlaps with section 6 in the use of QPE and projectors to address the computational complexity of Kronecker coefficients.

2 Background

We review some background which will be used in this paper. We start with a review of key properties of the group algebra $\mathbb{C}(S_n)$ of the symmetric group S_n and its centre $\mathcal{Z}(\mathbb{C}(S_n))$ which is the subspace that commutes with all elements of $\mathbb{C}(S_n)$. This is based on standard textbooks in group theory e.g. [41] and the relevant formulae are also collected in Appendices of recent physics papers such as [38, 32]. This is followed by a review of Quantum Phase Estimation (QPE) [7] algorithm from quantum computation.

2.1 The group algebra $\mathbb{C}(S_n)$ and its centre $\mathcal{Z}(\mathbb{C}(S_n))$

Let $\mathbb{C}(S_n)$ be the group algebra of the symmetric group S_n , i.e. the group algebra formed by linear combinations $\sum_{\sigma \in S_n} \lambda_\sigma \sigma$, $\lambda_\sigma \in \mathbb{C}$. Let $\mathcal{Z}(\mathbb{C}(S_n))$ be the center of $\mathbb{C}(S_n)$. There is a basis of $\mathcal{Z}(\mathbb{C}(S_n))$ formed by sums over group elements in conjugacy classes. Conjugacy classes in S_n are labelled by partitions μ of n (denoted $\mu \vdash n$). For a conjugacy class $\mathcal{C}_\mu \subset S_n$ we have a central element

$$T_\mu = \sum_{\sigma \in \mathcal{C}_\mu} \sigma. \quad (2.1)$$

obeying $\gamma T_\mu \gamma^{-1} = T_\mu$, for any $\gamma \in S_n$. We are interested, in particular, in conjugacy classes $\mu = [k, 1^{n-k}]$ defined by a single cycle of length k and all remaining cycles of length 1. These central elements have the form

$$\begin{aligned} T_2 &= \frac{1}{2} \sum_{1 \leq i_1 \neq i_2 \leq n} (i_1 i_2) = (12) + (13) + \dots \\ T_3 &= \frac{1}{3} \sum_{1 \leq i \neq j \neq k \leq n} ((ijk) + (ikj)) = (123) + (132) + (124) + (142) + \dots \\ &\vdots \\ T_k &= \frac{1}{k} \sum_{1 \neq i_1 \neq i_2 \dots \neq i_k} (i_1 i_2 \dots i_k) \end{aligned} \quad (2.2)$$

where the cycles of length 1 are not shown. We will refer to the T_k as cycle central elements in $\mathcal{Z}(\mathbb{C}(S_n))$.

The product of two general central elements for $\mu, \nu \vdash n$ yields

$$T_\mu T_\nu = \sum_{\lambda} C_{\mu\nu}^\lambda T_\lambda \quad (2.3)$$

where the integer structure constants $C_{\mu\nu}^\lambda$ can be organized as a matrix C_μ with matrix elements :

$$(C_\mu)_\nu^\lambda = C_{\mu\nu}^\lambda. \quad (2.4)$$

It is known that the eigenvalues of $(C_\mu)_\nu^\lambda$ are the normalized characters $\widehat{\chi}^R(T_\mu) := \frac{\chi^R(T_\mu)}{d_R}$ in the irrep labelled by the Young diagram $R \vdash n$ of dimension d_R .

Another basis for $\mathcal{Z}(\mathbb{C}(S_n))$ is given by the projectors P_R labelled by irreducible representations R (corresponding to Young diagrams with n boxes, i.e. $R \vdash n$):

$$P_R = \frac{d_R}{n!} \sum_{\sigma \in S_n} \chi^R(\sigma) \sigma \quad (2.5)$$

The multiplication of the conjugacy class elements with the projectors gives

$$T_\mu P_R = \widehat{\chi}^R(T_\mu) P_R \quad (2.6)$$

where $\widehat{\chi}^R(T_\mu)$ is the normalized character obtained by dividing the trace of the matrix $D^R(T_\mu)$ representing T_μ in the irrep R by the dimension d_R

$$\widehat{\chi}^R(T_\mu) = \frac{\chi^R(T_\mu)}{d_R} = \frac{\text{tr}(D^R(T_\mu))}{d_R} \quad (2.7)$$

Therefore, the linear operator of multiplication by T_μ in $\mathcal{Z}(\mathbb{C}(S_n))$, with matrix elements $(C_\mu)_\nu^\lambda$, has eigenvectors P_R associated with the eigenvalue $\widehat{\chi}^R(T_\mu)$. We will consider

$$\chi_\mu^{\max} = \max_{R \vdash n} \widehat{\chi}^R(T_\mu) \quad (2.8)$$

as a normalization factor such that the magnitude of eigenvalue of T_μ / χ_μ^{\max} associated with P_R is bounded by 1, as required by the QPE procedure.

The set of central elements $\{T_2, T_3, \dots, T_n\}$ multiplicatively generate the centre, i.e. linear combinations of these and their powers linearly span the centre $\mathcal{Z}(\mathbb{C}(S_n))$, while in fact subsets $\{T_2, \dots, T_{k_*(n)}\}$ with $k_*(n) < n$ generically form multiplicative sets of generators [25]. This is related to the fact that the ordered list of normalized characters $(\widehat{\chi}^R(T_2), \widehat{\chi}^R(T_3), \dots, \widehat{\chi}^R(T_{k_*(n)}))$ uniquely identifies the Young diagram R . The connection between such ordered lists and sets of multiplicative generators is reviewed and extended to general groups in [42]. The sequence $k_*(n)$ was explicitly computed, with the help of character formulae in [43, 44]. Here are some values of $k_*(n)$ for lower values of n up to 79:

$$\begin{aligned} k_*(n) &= 2 \text{ for } n \in \{2, 3, 4, 5, 7\} \\ k_*(n) &= 3 \text{ for } n \in \{6, 8, 9, \dots, 14\} \\ k_*(n) &= 4 \text{ for } n \in \{15, 16, \dots, 23, 25, 26\} \\ k_*(n) &= 5 \text{ for } n \in \{24, 27, \dots, 41\} \\ k_*(n) &= 6 \text{ for } n \in \{42, \dots, 78, 79, 81\} \end{aligned} \quad (2.9)$$

2.1.1 A heuristic argument for the asymptotics of $k_*(n)$ at large n

A necessary condition for the eigenvalues of $\{T_2, T_3, \dots, T_k\}$ to be able to distinguish all Young diagrams is that the number of distinct lists of eigenvalues exceeds the number of Young diagrams. The maximum eigenvalue of T_2 is $n(n-1)/2 \sim n^2$. These eigenvalues are integers. The number of possible eigenvalues is order n^2 . For T_3 we have order n^3 , and T_k order n^k as long as $k \ll n$. The total number of distinct eigenvalue lists is approximately

$$n^2 \times n^3 \cdots \times n^k = n^{k(k+1)/2} \quad (2.10)$$

A heuristic estimate for k_* is given by

$$n^{k_*(k_*+1)/2} = e^{\sqrt{n}} \quad (2.11)$$

Then

$$k_*(n)(k_*(n) + 1)/2 \log n = \sqrt{n} \quad (2.12)$$

Approximately at large n ,

$$k_*(n) \sim \frac{n^{1/4}}{\log n} \in n^{1/4} \quad (2.13)$$

Based on this heuristic argument, we conjecture that $k_*(n) \in \mathcal{O}(n^{1/4})$. For our main claim of a polynomial complexity of the QPE-based algorithms we describe subsequently the precise exponent is not important. It suffices that $k_*(n) \in \mathcal{O}(n^\alpha)$ with $\alpha < 1/2$.

Notation: asymptotic behaviours. In the above and henceforth, we use the following notation: for two positive functions $f, g : \mathbb{N} \rightarrow \mathbb{R}^+$, $f \in \mathcal{O}(g)$, if it exists a constant $c > 0$, and an integer $n_0 \in \mathbb{N}$, such that $\forall n \geq n_0, f(n) \leq cg(n)$. We will equally use, for that relation, the shorthand notation $f \sim g$. Using a loose language, sometimes, we will say f is $\mathcal{O}(g)$.

2.1.2 $k_*(n)$, Casimirs of $U(N)$ and multipole moments

This problem of identifying a multiplicatively generating set of cycle central elements of the form $\{T_2, T_3, \dots, T_{k_*(n)}\}$ in $\mathcal{Z}(\mathbb{C}(S_n))$ is related to the problem of identifying Young diagrams with n boxes. There is a transformation giving a sequence of Casimirs of $U(N)$ of the form $\{C_2, C_3, \dots, C_k\}$ and in terms of a set of cycle central operators $\{T_2, T_3, \dots, T_k\}$. This transformation has been described in the literature on large N 2d Yang Mills theory [5, 45] and has been used to show that elements in the list $\{C_2, C_3, \dots, C_k\}$ can be expressed in terms of cycle operators with a cut-off at k [25]. The work [24] relates the Casimirs of $U(N)$ to multi-pole moments of LLM geometries. Therefore the task

of distinguishing LLM geometries corresponding to Young diagrams with n boxes can formally be accomplished with a cut-off $\Lambda(n)$ on the Casimirs with $\Lambda(n) = k_*(n)$. We are assuming $N > n$ where the Young diagram detection problem involves all Young diagrams with n boxes : the $U(N)$ constraint that the first column has length no greater than N is irrelevant. This equality $\Lambda(n) = k_*(n)$ will be used in section 4 where we describe a classical gravity analog of the projector detection task. There is a potential issue in that strictly speaking the validity of the semi-classical super-gravity solution in AdS5/CFT4 requires $n \sim N^2$. It is possible that this is not an issue for the identification of the highly supersymmetric LLM geometry itself, but only in questions related to fluctuations of the LLM geometry. Another possible scenario for physically justifying the semi-classical LLM calculation in section 4 is that the LLM plane may be relevant to a dimensionally reduced model of AdS/CFT, e.g. of the kind considered in the context of spin matrix theory [46].

2.1.3 Unitary operators

We introduce the following operators on $\mathbb{C}(S_n)$. Consider the linear conjugation operator $S : \mathbb{C}(S_n) \rightarrow \mathbb{C}(S_n)$ maps a linear combination $A = \sum_i c_i \sigma_i \in \mathbb{C}(S_n)$ to $S(A) := \sum_i c_i \sigma_i^{-1}$. We easily check that $S^2 = \text{id}$ and call S an involution. Let $\delta : \mathbb{C}(S_n)^{\times 2} \rightarrow \mathbb{C}$ be the symmetric bilinear pairing that acts on two group algebra elements $A = \sum_i c_i \sigma_i$ and $B = \sum_j c'_j \sigma_j$, as

$$\delta(A, B) = \sum_{i,j} c_i c'_j \delta(\sigma_i \sigma_j) \quad (2.14)$$

with $\delta(s) = 1$ if $\sigma = \text{id}$ and 0 otherwise. Note that δ is also extended by linearity to $\mathbb{C}(S_n)$ in the following. We then define a sesquilinear form on $\mathbb{C}(S_n)^{\times 2}$ by

$$g(A, B) = \delta(\overline{S(A)}, B), \quad (2.15)$$

where $\bar{x} \in \mathbb{C}$ stands for the complex conjugation. One checks that g is nondegenerate and therefore induces an inner product on $\mathbb{C}(S_n)$.

We recall a useful proposition and its proof from [32].

Proposition 1. *For any $\mu \vdash n$, T_μ is a Hermitian operator acting on $\mathbb{C}(S_n)$ endowed with its inner product g .*

Proof. We want to verify the identity $g(A, T_\mu B) = g(T_\mu A, B)$ for $A = \sum_i c_i \sigma_i$ and $B = \sum_j c'_j \sigma_j$. We have

$$\begin{aligned} g(A, T_\mu B) &= \sum_{i,j} \bar{c}_i c'_j \delta(S(\sigma_i) T_\mu \sigma_j) = \sum_{i,j} \bar{c}_i c'_j \delta(S(T_\mu \sigma_j) \sigma_i) = \sum_{i,j} \bar{c}_i c'_j \delta(S(\sigma_j) S(T_\mu) \sigma_i) \\ &= \sum_{i,j} \bar{c}_i c'_j \delta(S(\sigma_j) T_\mu \sigma_i) = \sum_{i,j} \bar{c}_i c'_j \delta(S(T_\mu \sigma_i) \sigma_j) = g(T_\mu A, B) \end{aligned} \quad (2.16)$$

where at an intermediate stage we use $S(AB) = S(B)S(A)$, $S(T_\mu) = T_\mu$, and $\delta(S(A)) = \delta(A)$. □

T_μ , as a hermitian operator, determines a unitary operator $U_\mu = e^{\frac{2\pi i}{\chi_\mu^{\max}} T_\mu}$ with phases given by the normalized characters $\widehat{\chi}^R(T_\mu)/\chi_\mu^{\max}$: $U_\mu = e^{\frac{2\pi i}{\chi_\mu^{\max}} T_\mu} P_R = e^{\frac{2\pi i}{\chi_\mu^{\max}} \widehat{\chi}^R(T_\mu)} P_R$. It is therefore natural to use QPE to estimate the phases of such unitaries. The next task uses QPE with C- U_μ -gates to identify the corresponding normalized characters $\widehat{\chi}^R(T_\mu)$ and from that addresses new questions.

2.2 Quantum Phase Estimation

We review in this section the QPE algorithm and its run time complexity. We use Nielsen and Chuang's notation, see section 5.2 in [7]. Readers with a background in quantum information theory may wish to skip this section and simply glance at the last paragraph of this section. Those with an AdS/CFT and mathematical physics background but little quantum information, like ourselves at the start of this project, will hopefully find it useful.

Consider a unitary operator U with an eigenstate $|\psi\rangle$ of eigenvalue $e^{2\pi i\lambda}$, for an unknown λ . QPE is a quantum algorithm that aims at approximating the value of λ . It uses oracles (black boxes) giving access to controlled- U^{2^j} ($C-U^{2^j}$ or shortly CU) operations, for some j , and capable of preparing an initial state $|\psi\rangle$. As in many quantum algorithms, the fast Fourier transform defines a key subroutine of QPE. Finally the last important step in the procedure is a measurement that will deliver an approximation of the phase with a defined error rate (tolerance). Figure 1 gives the standard quantum circuit that provides the different phases of the QPE. In the following we use a register space of t qbits, i.e. the dimension of that space is 2^t . Without loss of generality, the eigenvalue λ is chosen such that $\lambda \in [0, 1]$. For our applications of QPE in the upcoming sections, it will be the case that λ has an exact t -bit expansion, in which case, as we see shortly, the exact eigenvalue can be determined by QPE with probability 1.

QPE algorithm goes through the following steps:

(1) Initialize a state $|0\rangle^{\otimes t} \otimes |\psi\rangle$, apply the Hadamard-gates (H-gates) on the first register to get

$$|\psi\rangle_0 = \frac{1}{2^{t/2}}(|0\rangle + |1\rangle)^{\otimes t} |\psi\rangle = \frac{1}{2^{t/2}} \sum_{j=0}^{2^t-1} |j\rangle |\psi\rangle \quad (2.17)$$

where $|j\rangle$ is (the computational basis) written in binary representation as $|j_1 j_2 \dots j_t\rangle$ and $j = \sum_{l=1}^t j_l 2^{t-l}$. Recall that the Hadamard operator is expressed by $H = |+\rangle\langle 0| + |-\rangle\langle 1|$ where $|\pm\rangle = (1/\sqrt{2})(|0\rangle \pm |1\rangle)$.

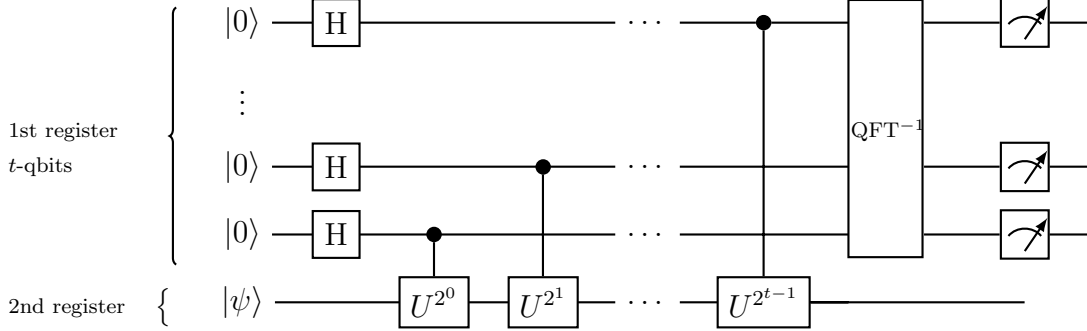


Figure 1: Quantum phase estimation by a quantum circuit acting on the initial state $|0\rangle^{\otimes t} \otimes |\psi\rangle$: H-boxes are Hadamard gates, U^{2^i} -boxes stand for CU-operators, $i = 0, \dots, t - 1$, QFT^{-1} for the inverse quantum Fourier transform, and the last stage involves a measurement on the first register.

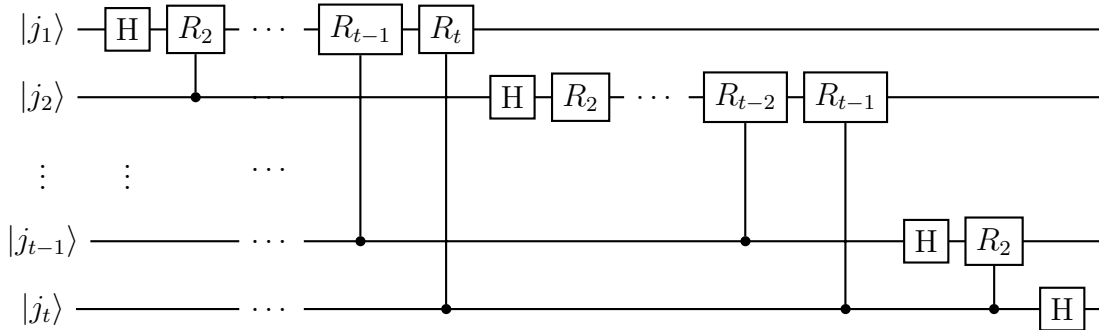


Figure 2: A circuit for quantum Fourier transform $|j_1 j_2 \dots j_t\rangle$: H-boxes are Hadamard gates, R_k -boxes stand for C- R_k -operators, $k = 2, \dots, t$.

(2) Apply the CU-gates (evolution operator):

$$|\psi_1\rangle = \left[\bigotimes_{i=1}^t C-U^{2^i} \right] |\psi\rangle_0 = \frac{1}{2^{t/2}} \sum_{j=0}^{2^t-1} e^{2\pi i j \lambda} |j\rangle |\psi\rangle \quad (2.18)$$

where each CU-gate is defined by $C-U^{2^i}(|0\rangle + |1\rangle)|\psi\rangle = |0\rangle|\psi\rangle + |1\rangle U^{2^i}|\psi\rangle$.

(3) Apply the inverse quantum Fourier transform (QFT⁻¹) to the first register of $|\psi_1\rangle$, with $C-R_k$ -operators defined by

$$R_k = \begin{pmatrix} 1 & 0 \\ 0 & e^{2\pi i/2^k} \end{pmatrix} \quad (2.19)$$

and obtain

$$|\psi_2\rangle = \frac{1}{2^t} \sum_{l=0}^{2^t-1} \sum_{j=0}^{2^t-1} e^{2\pi i j (\lambda - \frac{l}{2^t})} |l\rangle |\psi\rangle \quad (2.20)$$

Two cases may occur:

(a) suppose that λ has an exact t -bit expansion, there exists an l^* such that $l^*/2^t$ coincides with λ . The above expression takes the form

$$\begin{aligned} |\psi_2\rangle &= |l^*\rangle |\psi\rangle + \frac{1}{2^t} \sum_{l=0|l \neq l^*}^{2^t-1} \sum_{j=0}^{2^t-1} e^{2\pi i j (\lambda - \frac{l}{2^t})} |l\rangle |\psi\rangle \\ &= |l^*\rangle |\psi\rangle + \frac{1}{2^t} \sum_{l=0|l \neq l^*}^{2^t-1} \left[\frac{1 - e^{2\pi i (2^t \lambda - l)}}{1 - e^{2\pi i (\lambda - \frac{l}{2^t})}} \right] |l\rangle |\psi\rangle \\ &= |l^*\rangle |\psi\rangle + \frac{1}{2^t} \sum_{l=0|l \neq l^*}^{2^t-1} \left[\frac{1 - e^{2\pi i (l^* - l)}}{1 - e^{2\pi i (\lambda - \frac{l}{2^t})}} \right] |l\rangle |\psi\rangle \end{aligned} \quad (2.21)$$

the second term identically vanishes and we obtain

$$|\psi_2\rangle = |l^*\rangle |\psi\rangle \quad (2.22)$$

(4) Perform measurements of the t -bits in the first register. This yields $\lambda = l^*$ in binary form with probability 1.

(b) If λ does not have an exact t -bit expansion, then consider the best t -bit estimate b of λ : $b \in \llbracket 0, 2^t - 1 \rrbracket$ is the largest integer such that $b/2^t = b_1 2^{-1} + b_2 2^{-2} + \dots + b_t 2^{-t} < \lambda$. We define $\zeta = \lambda - b/2^t$, $0 < \zeta < 2^{-t}$, and write

$$|\psi_2\rangle = \frac{1}{2^t} \sum_{l=0}^{2^t-1} \sum_{j=0}^{2^t-1} e^{2\pi i j (\lambda - \frac{l}{2^t})} |l\rangle |\psi\rangle = \frac{1}{2^t} \sum_{l=0}^{2^t-1} \sum_{j=0}^{2^t-1} e^{2\pi i j (\zeta - \frac{(l-b)}{2^t})} |l\rangle |\psi\rangle$$

$$\begin{aligned}
&= \frac{1}{2^t} \sum_{l=0}^{2^t-1} \left[\frac{1 - e^{2\pi i(2^t \zeta - (l-b))}}{1 - e^{2\pi i(\zeta - \frac{l-b}{2^t})}} \right] |l\rangle |\psi\rangle \\
&= \frac{1}{2^t} \sum_{l=-b}^{2^t-1-b} \left[\frac{1 - e^{2\pi i(2^t \zeta - l)}}{1 - e^{2\pi i(\zeta - \frac{l}{2^t})}} \right] |l+b\rangle |\psi\rangle
\end{aligned} \tag{2.23}$$

Nielsen and Chuang mapped the amplitude of $|l+b\rangle|\psi\rangle$ to $\alpha_l \in \mathbb{C}$ defined in the following way:

$$\begin{aligned}
\alpha_l &\text{ is the amplitude of the state } |l+b\rangle \text{ labelled by } l = 0, 1, \dots, 2^t - 1 - b \tag{2.24} \\
\alpha_{2^t+l} &\text{ is the amplitude of the state } |l+b\rangle \text{ labelled by } l = -b, -b+1, \dots, -1
\end{aligned}$$

It is shown that $|\alpha_l| \leq 1/[2^{t+1}(\zeta - \frac{l}{2^t})]$ that will be useful to achieve the next probability bound.

(4') Perform measurements of the t -bits in the first register. It is proved (see section 5.2 in [7]) that the probability of getting b after a measurement m obeys the probability bound $P(|m-b| > e) < \epsilon = 1/(2(e-1))$, for a parameter $e = 2^{t-p} - 1 = 2^t \eta - 1$. Thus, if p is much smaller than t , e becomes large and induces a probability $P(|m-b| \leq e) \geq 1 - \epsilon$ close to 1.

Remarks. Although our present work solves a task that takes as input the eigenvectors of an evolution operator (which are projectors in an algebra), similar quantum algorithms to what we will present hereafter address other important questions and take superpositions of states as input (see discussion of the first future direction in section 6). Then, QPE can be implemented with any linear combination of eigenstates such as $|\Psi\rangle = \sum_{k=1}^n \beta_k |\psi_k\rangle$, for the eigenbasis $\{\psi_k\}$ of a Hermitian operator, and for coefficients $\beta_k \in \mathbb{C}$. Following step by step the previous algorithm, the end result takes the form

$$|\psi_2\rangle = \frac{1}{2^{t/2}} \sum_{l=0}^{2^t-1} \sum_{k=1}^n \beta_k \sum_{j=0}^{2^t-1} e^{2\pi i j(\lambda_k - \frac{l}{2^t})} |l\rangle |u_k\rangle \tag{2.25}$$

Consider a given eigenvalue λ_k approximated by the fraction $b_k/2^t$. After measurement, we obtain a probability $P(|m - b_k| > e) < |\beta_k|^2 \epsilon$ that remains small, for constant β_k . Thus, the procedures which follow here will adapt in this case and will remain accurate.

Complexity. The runtime complexities of QPE has been also discussed in [7]. The query complexity is $\mathcal{O}(t)$, as one requires t queries of the CU-operators. On the other hand, the gate complexity, that enumerates the number of gates used to deliver an output, is $\mathcal{O}(t^2)$ (t Hadamard gates, t CU-operators, the inverse QFT requires $t + (t-1) + \dots + 2 + 1$ H and $C-R_k$ gates, and therefore asymptotically leads to $\mathcal{O}(t^2)$ gates). Here and after, we summarize these statements as:

Query complexity $\in \mathcal{O}(t)$;

Gate complexity $\in \mathcal{O}(t^2)$.

In the projector detector tasks for algebras related to S_n which we consider in the following sections, where we will use unitary operators for QPE, which are exponentials of the cycle central operators discussed in section 2.1, we will be choosing the number of bits t to allow exact determination of the relevant eigenvalues which have known integrality properties. As a result this will translate into n -dependent complexities which are bounded by polynomials in n , subject to the assumption that $k_*(n) \in \mathcal{O}(n^\alpha)$ with $\alpha < 1/2$ which we described in section 2.1.1.

3 Quantum Phase Estimation for projectors in the centre of $\mathbb{C}(S_n)$

In this section, we focus on a quantum algorithm for detecting projectors in the centre $\mathcal{Z}(\mathbb{C}(S_n))$ of the group algebra $\mathbb{C}(S_n)$ of the symmetric group S_n . Bob prepares a projector P_R as a quantum state in the Hilbert space $\mathcal{Z}(\mathbb{C}(S_n))$. Alice is tasked with identifying the projector, i.e identifying the Young diagram R . Her procedure uses QPE to obtain the eigenvalues of appropriate Hermitian operators (the cycle central elements described in section 2.1) acting on the Hilbert space. These eigenvalues are expressible in terms of normalized characters of irreducible representations of S_n . We estimate the query and gate complexities of the algorithm using their standard definitions.

We are interested in particular in the cycle central elements T_k , $k \in \llbracket 1, n \rrbracket$, corresponding to partitions $\mu = [k, 1^{n-k}]$ with one cycle of length k and remaining cycles of length 1, described in more detail in section 2.1. Consider $U_k = e^{\frac{2\pi i}{\chi_k^{\max}} T_k}$ and $U_k P_R = e^{\frac{2\pi i}{\chi_k^{\max}} \widehat{\chi}^R(T_k)} P_R$, using the definition (2.8) for χ_k^{\max} . Alice's undertaking is the following :

TASK: Given the set of unitaries U_2, U_3, \dots, U_k , $k \in \llbracket 2, n \rrbracket$, and state P_R with unknown $R \vdash n$, determine which P_R we have.

We may imagine that Bob prepares the state P_R in $\mathcal{Z}(\mathbb{C}(S_n))$ and sends it to Alice who is tasked with the identification.

To answer this question, we will use QPE with $C - U_k$ -gates. We will subsequently compare with standard complexities of classical algorithms.

3.1 QPE for T_2

We restrict to this simplest (and non-trivial) case for a warm-up. We will use the known fact that [47]

$$\widehat{\chi}^R(T_2) = \frac{\chi^R(T_2)}{d_R} = \sum_{\square \in R} c(\square). \quad (3.1)$$

The sum is over boxes in the Young diagram R , weighted by the content of the box. The content is the column number minus the row number. The maximum value of the normalised character occurs for $R = [n]$, the Young diagram with a single row of n boxes. Then we have

$$\sum_{i=1}^n (i-1) = \frac{n(n-1)}{2} \quad (3.2)$$

The lowest value is $-n(n-1)/2$ and corresponds to $R = [1^n]$. Take for example $n = 6$, then $R = [6]$ gives $\widehat{\chi}^R(T_2) = 6 * 5/2 = 15$; for $R = [3, 2, 1]$, one has $\frac{\chi^R(T_2)}{d_R} = 0$. For $R = [2, 2, 2]$ it is -3 , for $R = [3, 3]$ it is 5 ; for $R = [4, 2]$ it is 5 . For simplicity, considering the value of $\widehat{\chi}^R(T_2)$, let us allow for all the integers between the bounds $-n(n-1)/2$ and $n(n-1)/2$.

The register must have enough bits to be able to store in binary all the numbers from $-n(n-1)/2$ to $n(n-1)/2$. This means the register has to be able to store $n(n-1) + 1$ possible integers. The number of bits needed is given by

$$t = \lceil \log_2(n(n-1) + 2) \rceil \in \mathcal{O}(\log n) \quad (3.3)$$

Thus, according to [7] (see Chapter 5.2), the QPE has complexities:

Query complexity $\in \mathcal{O}(t) = \mathcal{O}(\log(n))$;
Gate complexity $\in \mathcal{O}(t^2) = \mathcal{O}((\log(n))^2)$.

We now give an algorithm that will detect with probability 1, the projector P_R with a register of $t = \log n$ bits. $QPE(U_2)$ stands for the QPE with $C - U_2$ -operators. The query and gate complexities are the same as above.

3.2 General procedure for arbitrary n

From our previous discussion (particularly equation (2.2) and the associated remark (4)), we know that QPE can be done with certainty provided the eigenvalue can be exactly expressed with a t -bits. For instance, if $n \in \{2, 3, 4, 5, 7\}$, T_2 determines the projector P_R . However, for higher n , characterizing P_R will require access to more operators T_k 's as generating the centre $\mathcal{Z}(\mathbb{C}(S_n))$ requires more of these operators, see the discussion in subsection 2.1.

For $n \in \{6, 8, \dots, 14\}$, we need T_2, T_3 . Given a single copy of P_R , we can separately estimate the eigenvalues of T_2 and T_3 . To measure the eigenvalue of T_2 , in the exact way as above, Alice applies QPE for $U_2 = e^{\frac{2\pi i}{x_2^{\max}} T_2}$ using conditional unitaries C- U_2 . Using (2.2) the output of the first stage is P_R , tensored with some ancillary bits which are measured to give the eigenvalue $\widehat{\chi}^R(T_2)$ of T_2 . Then we apply QPE, using $U_3 = e^{\frac{2\pi i}{x_3^{\max}} T_3}$ and corresponding conditional unitaries C- U_3 -gates. The measure will give with certainty $\widehat{\chi}^R(T_3)$ of T_3 . The data pair $(\widehat{\chi}^R(T_2), \widehat{\chi}^R(T_3))$ determines in a unique way P_R by searching R in a table of size $2 * |\text{partitions}(n)|$.

For larger n , we simply iterate the procedure, enlarging the dimension of the register space and introducing a larger number of T_k , $k \in \llbracket 2, n \rrbracket$, that surely determine P_R . We need to perform the analysis at generic T_k , for $k \in \llbracket 2, n \rrbracket$.

3.2.1 Dimension of the register space for eigenvalues of general T_k

A first task is to collect the dimension of the register space associated with the calculation of the projector eigenvalues. We use a result on character bounds by Feray and Sniady [48]. They tell us that

$$\left| \frac{\chi_R(T_\mu)}{d_R} \right| \leq a |T_\mu| \left[\max\left(\frac{r(R)}{n}, \frac{c(R)}{n}, \frac{|\mu|}{n}\right) \right]^{|\mu|} \quad (3.4)$$

where a is a constant $a > 0$; $|\mu|$ is the minimum number of factors needed to write a permutation in T_μ as a product of transpositions; $r(R)$ is the number of rows; $c(R)$ is the number of columns in R . We observe that

$$\max\left(\frac{r(R)}{n}, \frac{c(R)}{n}, \frac{|\mu|}{n}\right) \leq \max\left(\frac{n}{n}, \frac{n}{n}, \frac{|\mu|}{n}\right) \leq 1 \quad (3.5)$$

using the fact that the number of rows and number of columns cannot exceed n . Thus, we have a bound

$$\left| \frac{\chi_R(T_\mu)}{d_R} \right| \leq a |T_\mu| \quad (3.6)$$

Dealing with $\mu = [k, 1^{n-k}]$, i.e. the case of interest associated with the cycle central elements T_k , we obtain the asymptotic behavior, for fixed k ,

$$\begin{aligned} \left| \frac{\chi_R(T_\mu)}{d_R} \right| &\leq a \frac{n(n-1) \cdots (n-k+1)}{k} = \frac{an^k}{k} \left(1 - \frac{1}{n}\right) \left(1 - \frac{2}{n}\right) \cdots \left(1 - \frac{k-1}{n}\right) \\ &\leq \frac{an^k}{k} \left(1 - \sum_{l=1}^{k-1} \frac{l}{n} + \text{terms vanishing at large } n\right) \\ &\leq \frac{an^k}{k} \left(1 - \frac{k(k-1)}{2n} + \text{terms vanishing at large } n\right) \end{aligned} \quad (3.7)$$

We are assuming that the cut-off $k_*(n)$ on the range of k needed obeys $k_*(n) \ll n$, which is certainly compatible with the conjecture $k_*(n) \in \mathcal{O}(n^{1/4})$ explained in section 2.1.1 but $k_*(n) \in \mathcal{O}(n^\alpha)$ for $\alpha < 1/2$ suffices to ensure that the second and higher terms in the expansion above are sub-leading at large n .

We also know [49] that $\frac{\chi_R(T_\mu)}{d_R}$ (for any partition μ) is an integer. So this means that the range of possible values of these eigenvalues is $2an^k$ and the smallest difference between eigenvalues is 1. Thus, on very general grounds, we can conclude that an upper bound on the number of bits required to encode all eigenvalues of the $C-U_k$ operators is given by

$$\begin{aligned} \text{Bits required to store eigenvalues of } T_k &\sim \log_2\left(2\frac{an^k}{k}\right) \\ &\sim \log_2(n^k) - \log_2 k \sim k \log n - \log k \end{aligned} \quad (3.8)$$

3.2.2 Query and gate complexities at general n

We will need to add the complexities for the measurements of $T_2, T_3, \dots, T_{k_*(n)}$. The total query complexity is estimated as

$$\begin{aligned} \sum_{k=2}^{k_*(n)} k \log(n) &= \left(\frac{k_*(n)(k_*(n)+1)}{2} - 1\right) \log(n) \\ \sum_{k=2}^{k_*(n)} (k \log(n) - \log(k)) &= \frac{k_*(n)(k_*(n)+1)}{2} \log(n) - \log(k_*(n)!) \\ &\sim \frac{k_*(n)(k_*(n)+1)}{2} \log(n) - k_*(n) \log(k_*(n)) \end{aligned} \quad (3.9)$$

If $k_*(n) < n^\alpha$ holds at large n , we have

$$t \sim \frac{k_*(n)(k_*(n)+1)}{2} \log(n) - k_*(n) \log(k_*(n)) \sim n^\alpha(n^\alpha - \alpha) \log n \sim n^{2\alpha} \log n \quad (3.10)$$

Thus, we obtain the

Query complexity $\in \mathcal{O}(t) \sim \mathcal{O}(n^{2\alpha} \log n)$.

For the gate complexity, we sum the number of gates required for each step and estimate

$$\sum_{k=2}^{k_*(n)} k^2 (\log(n))^2 \sim \frac{k_*(n)(k_*(n)+1)(2k_*(n)+1)}{6} (\log(n))^2 \quad (3.11)$$

If we use $k_*(n) = n^\alpha$ at large n , we obtain

Gate complexity $\in \mathcal{O}(n^{3\alpha} (\log n)^2)$. According to the heuristic conjecture in section 2.1.1, $\alpha = 1/4$, but for any $\alpha < 1/2$, the above gate and query complexities hold.

4 Classical algorithm related to quantum projector identification by holographic duality

Projectors in symmetric group algebras $\mathbb{C}(S_n)$ are used to construct half-BPS operators in $\mathcal{N} = 4$ super-Yang Mills theory with $U(N)$ gauge group, which is dual to string theory on $AdS_5 \times S^5$. These are composite operators built from n copies of a complex matrix Z . First we define

$$\mathcal{O}_\sigma(Z) = \sum_{i_1, \dots, i_n} Z_{i_{\sigma(1)}}^{i_1} \dots Z_{i_{\sigma(n)}}^{i_n} \quad (4.1)$$

This definition can be extended, by linearity, to include operators labelled by group algebra elements :

$$\mathcal{O}_{\sum_\sigma c_\sigma \sigma} = \sum_\sigma c_\sigma \mathcal{O}_\sigma(Z) \quad (4.2)$$

It then follows that for projectors

$$P_R = \frac{d_R}{n!} \sum_\sigma \chi^R(\sigma) \sigma \quad (4.3)$$

we have operators

$$\mathcal{O}_R = \frac{d_R}{n!} \sum_\sigma \chi^R(\sigma) \mathcal{O}_\sigma(Z) \quad (4.4)$$

Up to an unimportant normalization these are the standard Schur polynomial operators of the half-BPS Sector, which form an orthogonal basis for the free field inner product [12]. These states can be realized as holomorphic operators created by complex matrix oscillators arising from the $U(N)$ $\mathcal{N} = 4$ SYM theory reduced on $S^3 \times \mathbb{R}$. The dynamics of the reduced matrix model is isomorphic to that of a many-body system of N fermions in a one-dimensional harmonic oscillator potential [12, 50, 51]. Lin, Lunin and Maldacena [11] classified the half-BPS super-gravity solutions with $AdS_5 \times S^5$ asymptotics, which take the form:

$$ds^2 = -h^{-2} \left(dt + \sum_{i=1}^2 V_i dx_i \right)^2 + h^2 \left(dy^2 + \sum_{i=1}^2 dx_i dx_i \right) + R^2 d\Omega^2 + R^2 d\tilde{\Omega}^2 \quad (4.5)$$

The functions V_1, V_2, h, R appearing above are all functions of (x_1, x_2, y) , and are all determined by one function $u(x_1, x_2, y)$. The function obeys a harmonic equation in y and is determined by its value on the $y = 0$ plane.

In the papers [52, 24], the function $u(x_1, x_2)$ on the LLM plane is determined by using a Wigner phase space distribution associated to the quantum many-body fermion

state. This Wigner distribution arises from a reduced one-particle density matrix obtained from the many-body state by tracing out the states of $N - 1$ particles. The upshot of this discussion is eq. (25) from [24] which gives an expression for u that allows the determination of the conserved charges from the semi-classical geometry :

$$u(\rho, \theta) = 2 \cos^2 \theta \sum_{l=0}^{\infty} \frac{\sum_{f \in \mathcal{F}} A^l(f)}{\rho^{2l+2}} (-1)^l (l+1) {}_2F_1(-l, l+1; 1; \sin^2 \theta) \quad (4.6)$$

Here $\rho \in [0, \infty]$, $\theta \in [0, \frac{\pi}{2}]$, $\mathcal{F} = \{f_1, f_2, \dots, f_N\}$ a set of increasing integers related to the eigenvalues of individual Fermion $E_i = \hbar(f_i + \frac{1}{2})$, $i = 1, 2, \dots, N$. In such an expansion, $A^l(f)$ is a polynomial of order l in f (its explicit form can be found in [24]).

The relation between Jacobi polynomials and hypergeometrics will be useful (see [53])

$$P_n^{\alpha, \beta}(x) = \binom{\alpha + n}{n} {}_2F_1(-n, \alpha + \beta + n + 1; \alpha + 1; \frac{1-x}{2}) \quad (4.7)$$

Observe that we can match the hyper-geometric to the Jacobi polynomials by using

$$\begin{aligned} \alpha = 0, \quad \beta = 0, \quad n = l \\ \frac{1-x}{2} = \sin^2 \theta \implies x = \cos(2\theta) \end{aligned} \quad (4.8)$$

Then, under such a restriction, $u(\rho, \theta)$ (4.6) becomes

$$u(\rho, \theta) = 2 \cos^2 \theta \sum_{l=0}^{\infty} \frac{\sum_{f \in \mathcal{F}} A^l(f)}{\rho^{2l+2}} (-1)^l (l+1) P_l^{0,0}(\cos 2\theta) \quad (4.9)$$

Further useful information on Jacobi polynomials, including orthogonality relations, are given in [53].

Introducing, $X = \cos(2\theta)$, and a cut off Λ in l , we write an approximation of $u(\rho, \theta)$ at large enough Λ as

$$u(\rho, X, \Lambda) = (1 + X) \sum_{l=0}^{\Lambda} U(l, \rho) P_l^{0,0}(X) \quad (4.10)$$

where $U(l, \rho)$ given by

$$U(l, \rho) = \frac{\sum_{f \in \mathcal{F}} A^l(f)}{\rho^{2l+2}} (-1)^l (l+1) \quad (4.11)$$

The cut-off $\Lambda(n)$ is the cut-off on $U(N)$ Casimirs (for $N > n$) needed to ensure that the Young diagrams can be distinguished. As explained in section 2.1.2 it can be identified

with $k_*(n)$ which is defined intrinsically in terms of the symmetric group algebras $\mathbb{C}(S_n)$ and their centres $\mathcal{Z}(\mathbb{C}(S_n))$. The Casimirs of interest are given by

$$\sum_{f \in \mathcal{F}} A^l(f) = (-1)^l \rho^{2l+2} \frac{U(l, \rho)}{l+1} \quad (4.12)$$

and therefore can be extracted once we know $U(l, \rho)$. We define a reduced form of the function u by the equation

$$\tilde{u}(\rho, X, \Lambda) = \frac{u(\rho, X, \Lambda)}{(1+X)} = \sum_{l=0}^{\Lambda} U(l, \rho) P_l^{0,0}(X) \quad (4.13)$$

and this will be used in place of u .

Fast Fourier Transform (FFT) for $\tilde{u}(\rho, \theta, \Lambda)$. We use a well-established method, the FFT, to extract the coefficients $U(l, \rho)$ of $\tilde{u}(\rho, \theta, \Lambda)$. Our first task is to put $\tilde{u}(\rho, \theta, \Lambda)$ in a convenient form to apply the FFT algorithm.

We use the expansion of the Jacobi polynomial where $p_{l,k}^{0,0}$ is the coefficient in the expansion defined by the series (4.7), see [53]:

$$\begin{aligned} P_l^{0,0}(\cos 2\theta) &= \sum_{k=0}^l p_{l,k}^{0,0} (\cos 2\theta)^k \\ &= \sum_{k=0}^l p_{l,k}^{0,0} \frac{1}{2^k} \sum_{j=0}^k \binom{k}{j} e^{2i\theta(2j-k)} = \sum_{k=0}^l p_{l,k}^{0,0} \frac{1}{2^k} \sum_{\substack{m=-k \\ m+k \text{ even}}}^k \binom{k}{\frac{k+m}{2}} e^{2i\theta m} \\ &= \sum_{m=-l}^l \left[\sum_{\substack{k=|m| \\ m+k \text{ even}}}^l \frac{p_{l,k}^{0,0}}{2^k} \binom{k}{\frac{k+m}{2}} \right] e^{2i\theta m} = \sum_{m=-l}^l \tilde{p}_{l,m} e^{2i\theta m} \\ \tilde{p}_{l,m} &:= \sum_{\substack{k=|m| \\ m+k \text{ even}}}^l \frac{p_{l,k}^{0,0}}{2^k} \binom{k}{\frac{k+m}{2}} \end{aligned} \quad (4.14)$$

In the following, we will require access to the coefficients $\tilde{p}_{l,m}$ of the Jacobi polynomial $P_l^{0,0}$. Thus we use as input data table $\{\tilde{p}_{l,m}, l = 0, 1, \dots, \Lambda, m = -l, -l+1, \dots, l\}$.

Using (4.14), we reorganise the sum $\tilde{u}(\rho, \theta, \Lambda)$ in the following fashion

$$\begin{aligned} \tilde{u}(\rho, \theta, \Lambda) &= \sum_{l=0}^{\Lambda} U(l, \rho) \sum_{m=-l}^l \tilde{p}_{l,m} e^{2i\theta m} \\ &= \sum_{m=-\Lambda}^{\Lambda} \left[\sum_{l=|m|}^{\Lambda} U(l, \rho) \tilde{p}_{l,m} \right] e^{2i\theta m} = \sum_{m=-\Lambda}^{\Lambda} \tilde{C}_m(\rho, \Lambda) e^{2i\theta m} \end{aligned}$$

$$\tilde{C}_m(\rho, \Lambda) := \sum_{l=|m|}^{\Lambda} U(l, \rho) \tilde{p}_{l,m} \quad (4.15)$$

One can easily show that $\tilde{C}_m(\rho, \Lambda) = \tilde{C}_{-m}(\rho, \Lambda)$ which allows to return to a real expansion in $\cos(2m\theta)$. We focus on the values of $\tilde{C}_m(\rho, \Lambda)$, for $m = 0, \dots, \Lambda$. Suppose that we only have access to a finite number $\Lambda + 1$ of values of $\tilde{u}(\rho, \theta_l = \frac{\pi l}{\Lambda+1}, \Lambda)$, $l = 0, \dots, \Lambda$.

Then, the discrete Fourier transform (DFT) of $\tilde{u}(\rho, \theta, \Lambda)$ delivers the coefficients $\tilde{C}_m(\rho, \Lambda)$:

$$\begin{aligned} & \frac{1}{\Lambda+1} \sum_{l=0}^{\Lambda} \tilde{u}\left(\rho, \frac{\pi l}{\Lambda+1}, \Lambda\right) e^{-\frac{2i\pi l}{\Lambda+1}m} \\ &= \frac{1}{\Lambda+1} \sum_{l=0}^{\Lambda} \sum_{m'=-\Lambda}^{\Lambda} \tilde{C}_{m'}(\rho, \Lambda) e^{2i\frac{\pi l}{\Lambda+1}(m'-m)} \\ &= \frac{1}{\Lambda+1} \sum_{l=0}^{\Lambda} \left[\tilde{C}_m(\rho, \Lambda) + \sum_{m'=-\Lambda | m' \neq m}^{\Lambda} \tilde{C}_{m'}(\rho, \Lambda) e^{2i\frac{\pi l}{\Lambda+1}(m'-m)} \right] \\ &= \tilde{C}_m(\rho, \Lambda) + \frac{1}{\Lambda+1} \sum_{m'=-\Lambda | m' \neq m}^{\Lambda} \tilde{C}_{m'}(\rho, \Lambda) \frac{1 - e^{2i\frac{\pi(\Lambda+1)}{\Lambda+1}(m'-m)}}{1 - e^{2i\frac{\pi}{\Lambda+1}(m'-m)}} \\ &= \tilde{C}_m(\rho, \Lambda) \end{aligned} \quad (4.16)$$

The DFT has computational complexity $\mathcal{O}(\Lambda^2)$: we have order Λ coefficients to extract and order Λ multiplications (and additions of smaller complexity) to perform. Rather than doing a DFT, we perform a FFT to extract the coefficients $\tilde{C}_m(\rho, \Lambda)$ of $\tilde{u}(\rho, \theta, \Lambda)$. This is a classical algorithm, based on decimation-in-time, with $\Lambda = 2^r$ points, see e.g. [54], FFT decomposes the DFT in $r = \log_2 \Lambda$ steps, each of which generating $\Lambda/2$ basic computations called butterflies. In the end, FFT costs $\mathcal{O}(\Lambda \log \Lambda)$ basic operations.

The FFT delivers a table of values of $\tilde{C}_m(\rho, \Lambda)$, $m = 0, \dots, \Lambda$. We can then invert a linear system to obtain the $U(l, \rho)$:

$$\begin{aligned} \tilde{C}_\Lambda(\rho, \Lambda) &= U(\Lambda, \rho) \tilde{p}_{\Lambda, \Lambda} & U(\Lambda, \rho) &= \frac{1}{\tilde{p}_{\Lambda, \Lambda}} \tilde{C}_\Lambda(\rho, \Lambda) \\ \tilde{C}_{\Lambda-1}(\rho, \Lambda) &= \sum_{l=\Lambda-1}^{\Lambda} U(l, \rho) \tilde{p}_{l, \Lambda-1} = U(\Lambda-1, \rho) \tilde{p}_{\Lambda-1, \Lambda-1} + U(\Lambda, \rho) \tilde{p}_{\Lambda, \Lambda-1} \\ U(\Lambda-1, \rho) &= \frac{1}{\tilde{p}_{\Lambda-1, \Lambda-1}} \left[\tilde{C}_{\Lambda-1}(\rho, \Lambda) - U(\Lambda, \rho) \tilde{p}_{\Lambda, \Lambda-1} \right] \\ U(j, \rho) &= \frac{1}{\tilde{p}_{j, j}} \left[\tilde{C}_j(\rho, \Lambda) - \sum_{l=j+1}^{\Lambda} U(l, \rho) \tilde{p}_{l, j} \right] \\ j &= \Lambda-1, \Lambda-2, \dots, 0 \end{aligned} \quad (4.17)$$

We use the fact that the k th coefficient $p_{l,k}^{0,0}$ of the Jacobi polynomial $P_l^{0,0}$ expresses as (expand equation (1.1) of [53]):

$$p_{l,k}^{0,0} = \frac{(-1)^k}{l!} \sum_{m=k}^l \binom{l}{m} \binom{m}{k} \frac{(l+m)!}{2^m m!} (-1)^m \quad (4.18)$$

and thus the diagonal coefficient $\tilde{p}_{l,l} = \frac{(2l)!}{2^l (l!)^2}$ which is inverted in (4.17) does not vanish.

The above procedure accesses the table of values $\{\tilde{p}_{l,m}\}$, and depends on a parameter $\Lambda(n)$ which obeys $\Lambda(n) \in \mathcal{O}(n^\alpha)$. We assume that the computational complexity of measuring the $\tilde{u}(\rho, \theta_l = \frac{\pi l}{\Lambda+1}, \Lambda)$, $l = 0, \dots, \Lambda$, is bounded from above by a certain function $c_{\tilde{u}}(\Lambda)$, the complexity of measuring \tilde{u} at separations of $2\pi/(\Lambda+1)$. The estimation of $c_{\tilde{u}}(\Lambda)$ will require a complexity analysis of measurements in classical gravity, which we leave for future discussion and calculation.

Two procedures are involved above in the determination of the coefficients $U(l, \rho)$: a FFT and the resolution of the triangular linear system. The FFT has computational cost $\mathcal{O}(\Lambda \log \Lambda)$ and inverting this system costs $\mathcal{O}(\Lambda^2)$. Combining this yields a complexity $f(\Lambda)$ bounded from above by

$$f(\Lambda) \leq c_0 \Lambda c_{\tilde{u}}(\Lambda) + c_1 \Lambda \log \Lambda + c_2 \Lambda^2 \quad (4.19)$$

where c_0, c_1 and c_2 are constants. Hence, two sub cases could occur:

Case 1: if $c_{\tilde{u}}(\Lambda) \in \mathcal{O}(\Lambda^\beta)$ with $\beta \leq 1$, for large enough Λ , then the overall cost is $f(\Lambda) \in \mathcal{O}(\Lambda^2)$;

Case 2: if $c_{\tilde{u}}(\Lambda) \in \mathcal{O}(\Lambda^\beta)$ with $\beta > 1$ for large enough Λ and for some constant $c_0 > 0$, then $f(\Lambda)$ will be dominated by the cost of the measurement procedure $\mathcal{O}(\Lambda^{1+\beta})$.

In first case 1.1, we have the FFT and linear system inversion that are combined to give a complexity $f(\Lambda) \in \mathcal{O}(\Lambda^2) \sim \mathcal{O}(n^{2\alpha})$. Comparing to the QPE query and gate complexities given by $\mathcal{O}(n^{2\alpha} \log n)$, and $\mathcal{O}(n^{3\alpha} (\log n)^2)$, respectively, the classical holographic procedure has a better efficiency at large n . In case 1.2, if $1 < \beta \leq 2$, QPE query complexity is smaller than the holographic complexity, but the QPE gate complexity is larger. If $\beta > 2$, QPE has both query and gate complexities smaller than the holographic complexity.

It would be interesting to see if a more refined analysis would distinguish concepts of query and gate complexities during the determination of U in the holographic setting. There is another subtlety which is worth mentioning. It concerns the inversion of the linear system which may bring a limitation of the above conclusion. The coefficients $\tilde{p}_{l,m}$, for some large l and m , may have a size comparable to Λ^κ , for some positive integer κ . Therefore, we can use the fast Schonhage-Strassen multiplication or division by $\tilde{p}_{l,m}$ that costs $\mathcal{O}(\Lambda^\kappa \log \Lambda)$ [55] whenever we perform $U(l, \rho) \tilde{p}_{l,j}$ or divide by $\tilde{p}_{j,j}$. A more detailed analysis of κ would be needed to improve the comparison between the complexity

of detection of projector quantum states and the complexity of detection of geometries in the holographic dual. We leave these refinements for the future. The calculations in the present paper should be viewed as a proof of concept for the existence of meaningful comparisons of complexity between classical gravitational algorithms based on AdS and quantum algorithms based on CFT which are made possible by known holographic dualities. This is broadly aligned with the perspectives in [26, 27].

Note finally that one could be interested in solving the power sum moments $M_k = \sum_{i=1}^N f_i^k$. This can be also performed because of the relation $\sum_{f \in \mathcal{F}} A^l(f) = \sum_{k=0}^l c_k^l M_k$, for some coefficients c_k^l , see Appendix B. These relations can be recast as a triangular linear system that can be solved. For this reason, we take the view that knowing the $\sum_{f \in \mathcal{F}} A^l(f)$ is equivalent to knowing the M_k .

Future direction: Finite N effects.

In the above discussion, we have considered the complexity of the problem of detecting a Young diagram with n boxes from the set of all Young diagrams with n boxes. In $\mathcal{N} = 4$ SYM CFT this corresponds to considering the Young diagram basis for operators of dimension n . We have been able to formulate well-defined complexity estimation problems using the form of the function $u(\rho, \theta)$ determining the LLM solutions. An interesting extension of the complexity estimates given here is to consider the space of Young diagrams with N^2 boxes, for a large integer N , restricted to have the first column of length no greater than N . This is motivated by the condition of validity of the super-gravity approximation in describing the physics of high dimension CFT operators.

5 Classical matrix algorithms for projector detection: randomised classical algorithm

In section 4 we described a classical algorithm which related by holography to the quantum detection of projectors in section 3. A more conventional approach to classical/quantum comparison of algorithms is to use quantum-inspired randomised classical algorithms [29]. In this section we will develop such an approach for the projector detection task.

We can compare classical and quantum algorithms for this problem of detecting projector states. In the classical problem, we are given a set of matrices of size D , one matrix corresponding to every projector P_R . We can construct such matrices by taking the group algebra elements

$$P_R = \frac{d_R}{n!} \sum_{\sigma} \chi^R(\sigma) \sigma \tag{5.1}$$

in a reducible representation of dimension D . We need a reducible representation which, in its decomposition into irreducibles, contain every irrep R at least once.

We will work with the regular representation.

TASK 1 : The task of finding the T_2 eigenvalue

The input

- We are given, as a black-box which we can query, a projector P_R as a matrix $D^V(P_R)$ of size $\text{Dim}V \times \text{Dim}V$.
- We are also given, as a black box, a matrix $D^V(T_2)$.

Algorithm

- We query the $D^V(P_R)$ black box and ask for a pair of numbers (i, j) $1 \leq i, j \leq \text{Dim}V$ with a non-zero entry $(D^V(P_R))_{ij}$.
- We consider the matrix equation

$$(D^V(T_2)D^V(P_R))_{ij} = \sum_k (D^V(T_2))_{ik}(D^V(P_R))_{kj} = \frac{\chi^R(T_2)}{d_R}(D^V(P_R))_{ij} \quad (5.2)$$

We query the i 'th row $\{(D^V(T_2))_{ik} : k \in \{1, \dots, \text{Dim}V\}\}$ of the matrix $D^V(T_2)$ and the j 'th column $\{(D^V(P_R))_{kj} : k \in \{1, \dots, \text{Dim}V\}\}$ of $D^V(P_R)$.

- The sum over k in the equation (5.2) is computing a scalar product of two vectors. The two vectors are real. We will do the calculation of this inner product using a randomized classical algorithm (l_2 -norm sampling as in [29]). This will lead to a complexity which is independent of $\text{Dim}V$ and instead depends on the admissible error. This step is detailed below.
- By taking the ratio of $(D^V(T_2)D^V(P_R))_{ij}$ over $(D^V(P_R))_{ij}$ we can get the eigenvalue.

We now turn to the key computational step above is the multiplication of the i 'th row of $D^V(T_2)$ with the j 'th column $(D^V(P_R))_{ij}$. This is the computation of a dot-product of two vectors in dimension $\text{dim}V$. We can immediately apply known results in quantum-inspired classical algorithms . We use the result in Proposition 4.2 of [29], which gives the number of queries required to calculate the inner product of two vectors $\langle x, y \rangle$ with error $\epsilon \|x\| \|y\|$, and with success probability $(1 - \delta)$. The number of queries needed is $O(\frac{1}{\epsilon^2} \log(\frac{1}{\delta}))$. Here we are calculating $(T_2 P_R)_{ij}$ which is $\chi^R(T_2)/d_R$ times $(D^V(P_R))_{ij}$. We know the range of the normalized characters extends within the interval $[-n^2, n^2]$ and we know they are integers. From this we extract an estimate for the biggest ϵ we can afford. This will lead to query complexity which is polynomial in n , as we now show.

Let us consider the application of Proposition 4.2 of [29] to projectors in the regular representation.

Some important lemmas (to be proved in Appendix A) :

Lemma 1.

$$\sum_{\gamma} (D_{\gamma\mu}^{\text{reg}}(P_R))^2 = \frac{d_R^2}{n!} \quad (5.3)$$

Lemma 2.

$$\sum_{\tau} (D_{\sigma\tau}^{\text{reg}}(T_2))^2 = \frac{n(n-1)}{2} \quad (5.4)$$

Useful to choose fixed σ, μ with the property that $D_{\sigma\mu}^{\text{reg}}(P_R) \neq 0$. Then define vectors of dimension $n!$

$$\begin{aligned} X_{\gamma} &= D_{\gamma\mu}^{\text{reg}}(P_R) \\ Y_{\tau} &= D_{\sigma\tau}^{\text{reg}}(T_2) \end{aligned} \quad (5.5)$$

The above lemmas are telling us

$$\begin{aligned} \|X\|^2 &= \frac{d_R^2}{n!} \\ \|Y\|^2 &= \frac{n(n-1)}{2} \end{aligned} \quad (5.6)$$

Also we have

$$\begin{aligned} \langle X, Y \rangle &= \sum_{\gamma} (D_{\sigma\gamma}^{\text{reg}}(T_2)(D_{\gamma\mu}^{\text{reg}}(P_R)) \\ &= D_{\sigma\mu}^{\text{reg}}(T_2 P_R) \\ &= \frac{\chi^R(T_2)}{d_R} D_{\sigma\mu}^{\text{reg}}(P_R) \end{aligned} \quad (5.7)$$

Lemma 4.2 of [29] tells us that error

$$\Delta(\langle X, Y \rangle) = \epsilon \|X\| \|Y\| \quad (5.8)$$

can be achieved with query complexity $O(\frac{1}{\epsilon^2} \log \frac{1}{\delta})$, where δ is the failure probability to get within $\epsilon \|X\| \|Y\|$ of $\langle X, Y \rangle$. In the following, we neglect $\log \frac{1}{\delta}$ as it is independent of n . In the present application, we are taking $D_{\sigma\mu}^{\text{reg}}(P_R)$ to be given to us by an oracle, so it is an exactly known quantity. So we have

$$\Delta(\langle X, Y \rangle) = \Delta\left(\frac{\chi^R(T_2)}{d_R}\right) D_{\sigma\mu}^{\text{reg}}(P_R) \quad (5.9)$$

Equivalently, dividing by the known quantity $D_{\sigma\mu}^{\text{reg}}(P_R)$ we have

$$\Delta\left(\frac{\langle X, Y \rangle}{D_{\sigma\mu}^{\text{reg}}(P_R)}\right) = \Delta\left(\frac{\chi^R(T_2)}{d_R}\right) \quad (5.10)$$

We want this uncertainty to be less than 1 : then we can use the integrality property of the normalised characters to ensure that we can use the classical algorithm to detect the normalized character. If we set

$$\Delta\left(\frac{\chi^R(T_2)}{d_R}\right) = \epsilon \|X\| \|Y\| \leq 1 \quad (5.11)$$

we get

$$\epsilon \leq \frac{1}{\|X\| \|Y\|} = \sqrt{\frac{n!}{d_R^2}} \cdot \sqrt{\frac{2}{n(n-1)}} \sim \sqrt{\frac{n!}{d_R^2} \frac{1}{n}} \quad (5.12)$$

Let us call the upper bound on ϵ as ϵ^* . So we have

$$\epsilon^* = \sqrt{\frac{n!}{d_R^2} \frac{1}{n}} \quad (5.13)$$

This leads to a lower bound on the query complexity which we call Q^*

$$Q^*(R) = \frac{1}{(\epsilon^*)^2} = n^2 \cdot \frac{d_R^2}{(n!)} \quad (5.14)$$

This complexity is maximised for the largest d_R . There are easily derived bounds on the d_R^{max}

$$\sqrt{\frac{|G| - a(G)}{c(G) - a(G)}} \leq d_R^{max} \leq \sqrt{|G| - a(G)}. \quad (5.15)$$

as discussed in math-overflow [56]. Here $|G| = n!$, $c(G)$ is the number of conjugacy classes $p(n)$. $a(G)$ is the number of irreps of dimension 1. The only irreps having dimension 1 are the trivial and the anti-symmetric, so $a(G) = 2$. So we get

$$\frac{n! - 2}{(p(n) - 2)} \leq (d_R^{max})^2 \leq (n! - 2) \quad (5.16)$$

We conclude

$$Q^*(R_{max}) \leq n^2 \cdot \frac{(n! - 2)}{(n!)} \sim n^2 \quad (5.17)$$

TASK 2 : The task of finding the T_k eigenvalue for general $k \in \{2, 3, \dots, k_*(n)\}$

The input

- We are given, as black-box which we can query, a projector P_R as a matrix $D^V(P_R)$ of size $\text{Dim}V \times \text{Dim}V$.

- We are also given, as black boxes, the matrices $D^V(T_2), D^V(T_3), \dots, D^V(T_{k_*(n)})$

We apply the same previous algorithm successively for T_2, T_3, \dots , and $T_{k_*(n)}$.

We use the matrix of T_k in the regular representation, i.e. $D^{\text{reg}}(T_k)$ that should fulfil the following relation.

Lemma 3.

$$\sum_{\tau} (D_{\sigma\tau}^{\text{reg}}(T_k))^2 = \frac{n(n-1) \cdots (n-k+1)}{k} \quad (5.18)$$

Proof. Use the same steps as in proof of Lemma 2 in Appendix A, the above sum boils down to $\delta(T_k^2) = \sum_{c,c' \in \mathcal{C}_k} \delta(\sigma_c \sigma_{c'}) = |T_k| = n!/(k(n-k)!)$, where $\mathcal{C}_k = \{\sigma \in [k, 1^{n-k}]\}$ contains all permutation with cycle structure given by $[k, 1^{n-k}]$. \square

Using the regular representation, with $D_{\sigma\mu}^{\text{reg}}(P_R) \neq 0$, at step k , we define vectors of dimension $n!$

$$X_{\gamma} = D_{\gamma\mu}^{\text{reg}}(P_R), \quad Y_{\tau} = D_{\sigma\tau}^{\text{reg}}(T_k) \quad (5.19)$$

Lemmas 1 and 3 shows us that

$$\|X\|^2 = \frac{d_R^2}{n!}, \quad \|Y\|^2 = \frac{n(n-1) \cdots (n-k+1)}{k} \quad (5.20)$$

Computing the inner product, we obtain

$$\langle X, Y \rangle = \sum_{\gamma} D_{\sigma\gamma}^{\text{reg}}(T_k) D_{\gamma\mu}^{\text{reg}}(P_R) = D_{\sigma\mu}^{\text{reg}}(T_k P_R) = \frac{\chi^R(T_k)}{d_R} D_{\sigma\mu}^{\text{reg}}(P_R) \quad (5.21)$$

Using again Lemma 4.2 of [29], then the error $\Delta(\langle X, Y \rangle) = \epsilon \|X\| \|Y\|$ can be achieved with query complexity $O(\frac{1}{\epsilon^2})$ (neglecting the failure probability δ). As $D_{\sigma\mu}^{\text{reg}}(P_R)$ is queried by an oracle, we have

$$\Delta(\langle X, Y \rangle) = \Delta\left(\frac{\chi^R(T_k)}{d_R}\right) D_{\sigma\mu}^{\text{reg}}(P_R) \quad (5.22)$$

Dividing by $D_{\sigma\mu}^{\text{reg}}(P_R)$, one gets

$$\Delta\left(\frac{\langle X, Y \rangle}{D_{\sigma\mu}^{\text{reg}}(P_R)}\right) = \Delta\left(\frac{\chi^R(T_k)}{d_R}\right) \quad (5.23)$$

We want this uncertainty to be less than 1: then, by the same routine that ensures us that we can use the classical algorithm to detect the normalized character, we set

$$\Delta\left(\frac{\chi^R(T_k)}{d_R}\right) = \epsilon \|X\| \|Y\| \leq 1 \quad (5.24)$$

and obtain, for $k \ll n$

$$\epsilon \leq \frac{1}{\|X\| \|Y\|} = \sqrt{\frac{n!}{d_R^2}} \cdot \sqrt{\frac{k}{n(n-1)\dots(n-k+1)}} \sim \sqrt{\frac{n!}{d_R^2}} \sqrt{\frac{k}{n^k}} \quad (5.25)$$

Making use of the upper bound ϵ^* on ϵ , we write a lower bound on the query complexity which we call Q_k^*

$$Q_k^*(R) = \frac{1}{(\epsilon^*)^2} = \frac{n^k}{k} \cdot \frac{d_R^2}{(n!)} \quad (5.26)$$

which holds for $k = 2, 3, \dots, k_*(n)$. Taking the worst case, this complexity is maximised for the largest d_R . Keeping in mind $(d_R^{\max})^2 \leq (n! - 2)$ (5.15), we are led to

$$Q_k^*(R_{\max}) \leq \frac{n^k}{k} \cdot \frac{(n! - 2)}{(n!)} \sim \frac{n^k}{k} \quad (5.27)$$

This is the behavior of the largest query complexity for each k . The total query complexity is obtained by summing them:

$$Q^*(R_{\max}) = \sum_{k=2}^{k_*(n)} Q_k^*(R_{\max}) = \sum_{k=2}^{k_*(n)} \frac{n^k}{k} \geq \frac{n^{k_*(n)}}{k_*(n)} = n^{n^\alpha - \alpha} \quad (5.28)$$

where we assume $k_*(n) = \mathcal{O}(n^\alpha)$ at large n (for some $0 < \alpha < 1/2$, with $\alpha = 1/4$ being a conjecture as discussed in section (2.1)). This shows that the query complexity of this algorithm is much larger than that of the quantum algorithm with $n^{2\alpha} \log n$, see (3.10).

5.1 Discussion and future directions

5.1.1 Interpretation

We are finding, for the Young diagram projector detection task, that the quantum phase estimation methods perform exponentially better than the classical analog we have defined using randomised algorithms (compare for example (3.3) with (5.17)). This may be due to the intrinsically quantum nature of our task which may bring it closer to the exponential quantum improvements envisioned in [57]. There is no computational cost of converting classical vector data to quantum states in our discussion of section 3. In practical recommendation tasks it has been found that the randomised algorithms only differ polynomially in complexity from the quantum tasks [58][29].

5.1.2 One dimensional representations

We have asserted, in arriving at (5.16), that the one-dimensional representations of the symmetric groups are the trivial and the sign representations. That there are no further one-dimensional irreps over \mathbb{C} for S_n ($n \geq 2$) is discussed in [59] [60] [61].

5.1.3 More general choices of V .

We have formulated the randomised classical algorithm in terms of the regular representation. We could also use a more general reducible representation which contains all irreps R in its decomposition into irreducibles. If V contains every irrep R , then its dimension is at least

$$\sum_R d_R \tag{5.29}$$

It is known that this sum is equal to the number of permutations σ which square to 1. This means that σ only has one and two-cycles. Let k be the number of 2-cycles.

$$\sum_R d_R = \sum_{k=0}^{\lfloor \frac{n}{2} \rfloor} \frac{n!}{2^k k! (n-2k)!} \tag{5.30}$$

The summand is maximum when $k = (n/2)$. The value is then

$$\frac{n!}{(n/2)! 2^{n/2}} \tag{5.31}$$

A lower bound is therefore

$$D_- = \frac{n!}{(n/2)! 2^{n/2}} \tag{5.32}$$

An upper bound is

$$D_+ = (n/2) D_- \tag{5.33}$$

6 Detection of the Kronecker projector in $\mathcal{K}(n)$

Permutation centralizer algebras $\mathcal{K}(n)$ related to $\mathbb{C}(S_n)$, which arise in the enumeration of tensor model observables and the computation of their correlators [62, 31] have been used to give constructive integer matrix algorithms for computing Kronecker coefficients [32, 63]. These algorithms are based on regarding $\mathcal{K}(n)$ as Hilbert spaces. The dimensions of these Hilbert spaces grow as $n!$ at large n (see [64] for all orders asymptotic formulae for these dimensions). An important motivation for this paper has been to take

advantage of known exponential improvements due to quantum algorithms [57] to formulae efficient algorithms based on $\mathcal{K}(n)$ for Kronecker coefficients, since an important element of the interest in Kronecker coefficients comes from computational complexity theory [65, 66, 67, 68]. Our perspective is that, while the intersection of representation theory in mathematics and computational complexity in computer science is a fascinating interface with many interesting outcomes, the mathematical question of combinatorial constructibility of representation theory quantities is sometimes fruitfully kept distinct from the complexity theoretic questions associated with the precise choice of computational task based on Kronecker coefficients and the efficiency of algorithms for the chosen task. Informally speaking we would argue that construction problems, such as making hay and manufacturing needles, are distinct from complexity questions, such as the difficulty of finding a needle in a haystack. We review the basics of $\mathcal{K}(n)$ from [31] and apply QPE to projector detection task in $\mathcal{K}(n)$. The projector is labelled by a triple of Young diagrams with non-vanishing coefficient.

Consider $\mathbb{C}(S_n) \otimes_{\mathbb{C}} \mathbb{C}(S_n)$, simply denoted $\mathbb{C}(S_n) \otimes \mathbb{C}(S_n)$. Introduce the tensor product elements $\sigma_1 \otimes \sigma_2$ and sum over all their diagonal conjugates as

$$\sigma_1 \otimes \sigma_2 \rightarrow \sum_{\gamma \in S_n} \gamma \sigma_1 \gamma^{-1} \otimes \gamma \sigma_2 \gamma^{-1} \quad (6.1)$$

Now, consider the \mathbb{C} -vector subspace $\mathcal{K}(n) \subset \mathbb{C}(S_n) \otimes \mathbb{C}(S_n)$ spanned by all $\sum_{\gamma \in S_n} \gamma \sigma_1 \gamma^{-1} \otimes \gamma \sigma_2 \gamma^{-1}$, σ_1 and $\sigma_2 \in S_n$:

$$\mathcal{K}(n) = \text{Span}_{\mathbb{C}} \left\{ \sum_{\gamma \in S_n} \gamma \sigma_1 \gamma^{-1} \otimes \gamma \sigma_2 \gamma^{-1}, \sigma_1, \sigma_2 \in S_n \right\} \quad (6.2)$$

The dimension of $\mathcal{K}(n)$ maps to the number of ribbon graphs with n edges, and equivalently to a sum over triples R_1, R_2, R_3 of irreducible representations (irreps) of S_n [31]:

$$|\text{Rib}(n)| = \text{Dim}(\mathcal{K}(n)) = \sum_{R_1, R_2, R_3 \vdash n} C(R_1, R_2, R_3)^2 \quad (6.3)$$

The Kronecker coefficient $C(R_1, R_2, R_3)$ is a non-negative-integer that yields the number of times R_3 appears in the tensor product decomposition $R_1 \otimes R_2$. The Kronecker coefficient is expressed in terms of characters as

$$C(R_1, R_2, R_3) = \frac{1}{n!} \sum_{\sigma \in S_n} \chi_{R_1}(\sigma) \chi_{R_2}(\sigma) \chi_{R_3}(\sigma) \quad (6.4)$$

In an analogous way of section 3, there are operators that multiplicatively generate the centre of $\mathcal{K}(n)$. At any $n \geq 2$, we define elements in $\mathbb{C}(S_n) \otimes \mathbb{C}(S_n)$

$$T_k^{(1)} = T_k \otimes 1 = \sum_{\sigma \in \mathcal{C}_k} \sigma \otimes 1,$$

$$\begin{aligned}
T_k^{(2)} &= 1 \otimes T_k = \sum_{\sigma \in \mathcal{C}_k} 1 \otimes \sigma, \\
T_k^{(3)} &= \sum_{\sigma \in \mathcal{C}_k} \sigma \otimes \sigma.
\end{aligned} \tag{6.5}$$

The sum of products of the $T_k^{(i)}$'s, $k = 1, \dots, n$, generates the centre $\mathcal{Z}(\mathcal{K}(n))$ of $\mathcal{K}(n)$. In fact, one does not need the entire set $k = 1, \dots, n$ to generate the centre, only a fewer number of them is enough $k = 1, \dots, k_*(n) \leq n$.

$\mathcal{K}(n)$ has a matrix basis

$$Q_{\tau_1, \tau_2}^{R_1, R_2, R_3} = \frac{d_{R_1} d_{R_2}}{(n!)^2} \sum_{\tau=1}^{C(R_1, R_2, R_3)} \sum_{\sigma_1, \sigma_2 \in S_n} \sum_{i_1, i_2, i_3, j_1, j_2} C_{i_1, i_2, i_3}^{R_1, R_2, R_3, \tau_1} C_{j_1, j_2, i_3}^{R_1, R_2, R_3, \tau_2} D_{i_1 j_1}^{R_1}(\sigma_1) D_{i_2 j_2}^{R_2}(\sigma_2) \sigma_1 \otimes \sigma_2 \tag{6.6}$$

obeying

$$Q_{\tau_1, \tau_2}^{R_1, R_2, R_3} Q_{\tau'_1, \tau'_2}^{R'_1, R'_2, R'_3} = \delta^{R_1, R'_1} \delta^{R_2, R'_2} \delta^{R_3, R'_3} \delta_{\tau_2, \tau'_1} Q_{\tau_1, \tau'_2}^{R_1, R_2, R_3} \tag{6.7}$$

$D_{ij}^R(\sigma)$ are the matrix elements of the linear operator $D^R(\sigma)$ in an orthonormal basis for the irrep R . The index τ runs over an orthonormal basis for the multiplicity space of dimension equals to the Kronecker coefficient $C(R_1, R_2, R_3)$. κ_{R_1, R_2, R_3} is a normalization factor. $C_{i_1, i_2, i_3}^{R_1, R_2, R_3, \tau_1}$ are Clebsch-Gordan coefficients of the representations of S_n (see the appendices of [31] for the properties needed to prove that this expression gives a Wedderburn-Artin basis for $\mathcal{K}(n)$).

The centre $\mathcal{Z}(\mathcal{K}(n))$ is spanned by

$$P^{R_1, R_2, R_3} = \sum_{\tau} Q_{\tau, \tau}^{R_1, R_2, R_3}$$

This is equal to an expression in terms of characters

$$\begin{aligned}
\tilde{P}^{R_1, R_2, R_3} &= \Delta(P_{R_3})(P_{R_1} \otimes P_{R_2}) \\
&= \frac{1}{(n!)^3} d_{R_1} d_{R_2} d_{R_3} \sum_{\sigma_1, \sigma_2, \sigma_3 \in S_n} \chi^{R_1}(\sigma_1) \chi^{R_2}(\sigma_2) \chi^{R_3}(\sigma_3) \sigma_3 \sigma_1 \otimes \sigma_3 \sigma_2
\end{aligned} \tag{6.8}$$

The equality $P^{R_1, R_2, R_3} = \tilde{P}^{R_1, R_2, R_3}$ can be shown using the properties :

$$\begin{aligned}
P^{R'_1} \tilde{P}^{R_1, R_2, R_3} &= \delta^{R_1, R'_1} \tilde{P}^{R_1, R_2, R_3} \\
P^{R'_2} \tilde{P}^{R_1, R_2, R_3} &= \delta^{R_2, R'_2} \tilde{P}^{R_1, R_2, R_3} \\
P^{R'_3} \tilde{P}^{R_1, R_2, R_3} &= \delta^{R_3, R'_3} \tilde{P}^{R_1, R_2, R_3} \\
\tilde{P}^{R_1, R_2, R_3} \tilde{P}^{R'_1, R'_2, R'_3} &= \delta^{R_1, R'_1} \delta^{R_2, R'_2} \delta^{R_3, R'_3} \tilde{P}^{R_1, R_2, R_3}
\end{aligned} \tag{6.9}$$

It is known that, as (R_1, R_2, R_3) range over triples of Young diagrams with non-vanishing Kronecker coefficient, and τ_1, τ_2 each range over a basis for the Kronecker multiplicity space, the elements $Q_{\tau_1, \tau_2}^{R_1, R_2, R_3}$ form a basis for $\mathcal{K}(n)$ [32]. The above equations imply that

$$\tilde{P}^{R_1, R_2, R_3} = \sum_{\tau} a_{\tau} Q_{\tau, \tau}^{R_1, R_2, R_3} \quad (6.10)$$

Further we show, in Appendix C, that for any fixed τ ,

$$\tilde{P}^{R_1, R_2, R_3} Q_{\tau, \tau}^{R_1, R_2, R_3} = Q_{\tau, \tau}^{R_1, R_2, R_3} \quad (6.11)$$

Along with the use of the inner product on $\mathcal{K}(n)$ (described in [32]) this equation implies that $\tilde{P}^{R_1, R_2, R_3} = P^{R_1, R_2, R_3}$.

SET-UP: Bob sends to Alice a non-vanishing projector P^{R_1, R_2, R_3} associated with a triple (R_1, R_2, R_3) with non-vanishing Kronecker coefficient. Alice is asked to detect the triple of Young diagrams labelling the projector.

Alice uses successive phase estimations with $U_{k,i} = e^{\frac{2\pi i}{\chi_k^{\max}} T_k^{(i)}}$, for $i \in \{1, 2, 3\}$ and $k \in \{1, 2, \dots, k_*(n)\}$. For each k, i we have a certain number of black-box queries in QPE (for the controlled U -gates) and a number of gates for inverse quantum Fourier transformation. We add up all the gates to get the gate complexity and all the black box queries to get the query complexity.

TASK: Identify a triple (R_1, R_2, R_3) for a Kronecker projector P^{R_1, R_2, R_3}

Consider the set of unitaries $U_{k,i} = e^{\frac{2\pi i}{\chi_k^{\max}} T_k^{(i)}}$, for any i and k , that satisfy $U_{k,i} P^{R_1, R_2, R_3} = e^{\frac{2\pi i}{\chi_k^{\max}} \chi^{R_i}(T_k^{(i)})} P^{R_1, R_2, R_3}$. The problem is formulated as follows:

“Given the set of unitaries $U_{2,i}, U_{3,i}, \dots, U_{k,i}$, $i = 1, 2, 3$, $k \in \llbracket 2, k_*(n) \rrbracket$, and state P^{R_1, R_2, R_3} with unknown $R_i \vdash n$, $i = 1, 2, 3$, determine which P^{R_1, R_2, R_3} we have.”

The reasoning is analogous of the previous section 3. The number of bits require to store de top eigenvalue of $T_k^{(i)}$ for any i and k is known (7.8). The query complexity adds the number of queries of all $C-U_{k,i}$ -operators

$$\sum_{i=1}^3 \sum_{k=2}^{k_*(n)} k \log(n) = 3 \left(\frac{k_*(n)(k_*(n) + 1)}{2} - 1 \right) \log(n) \quad (6.12)$$

Using again $k_*(n) = n^{\alpha}$, we obtain

Query complexity $\in \mathcal{O}(t) \sim \mathcal{O}(n^{2\alpha} \log n)$.

In a similar way, the gate complexity sums the number of gates required for each step and estimate

$$\sum_{i=1}^3 \sum_{k=2}^{k_*(n)} k^2 (\log(n))^2 \sim k_*(n)^3 (\log(n))^2 \quad (6.13)$$

If we use $k_*(n) = n^\alpha$ and at large n , this boils down to **Gate complexity** $\in \mathcal{O}(n^{3\alpha}(\log n)^2)$.

Future directions

Generating list of triples with non-vanishing Kronecker coefficients

We have presented complexity estimates for the detection of Kronecker projectors which exist for every triple of Young diagrams having non-vanishing Kronecker coefficients. A natural next step in understanding Kronecker coefficients in the context of ribbon graph quantum mechanics is to consider the ribbon graph corresponding to state in $\mathcal{K}(n)$ corresponding to the permutation pairs $(\sigma_1 = \sigma_0, \sigma_2 = \sigma_0)$ where σ_0 is the identity permutation. When this is expanded in the Fourier basis, we get a linear combination with non-vanishing coefficients of the projector states P^{R_1, R_2, R_3} for all the triples (R_1, R_2, R_3) having non-vanishing Kronecker coefficients. The application of QPE with the operators $U_{k,i}$ will be able to produce the list of Young diagram triples with non-vanishing Kroneckers. We leave the complexity estimates for this task to the future.

Detecting whether the Kronecker coefficient for a triple is greater than 1

By focusing on the detection of the projector states P^{R_1, R_2, R_3} in $\mathcal{K}(n)$ we have explained algorithms for identifying/detecting specific triples from the set of all triples with non-vanishing Kronecker coefficient. Making use of the more refined structure of $\mathcal{K}(n)$, notably its Wedderburn-Artin decomposition in terms of $Q_{\tau_1, \tau_2}^{R_1, R_2, R_3}$ would allow access to generalisations of this task. For example Bob could send Alice a pair of Q -states, both with the same (R_1, R_2, R_3) and with Kronecker coefficient 1 or greater than 1, and Alice could be tasked with determining the triple of Young diagrams and determining whether the two states sent by Bob are linearly independent. If they are, then this would show that the Kronecker coefficient for the triple is greater than 1. This would require using QPE to determine the eigenvalues of elements in $\mathcal{K}(n)$ which are not necessarily central. The use of non-central elements of a permutation centraliser algebra to construct distinct multiplicity states (τ_1, τ_2) has been used [37] in the context of multi-matrix invariants (related to the algebra $\mathcal{A}(m, n)$ discussed in section 7).

Holography

Following the similarity between the projector detection in this section and the detection in $\mathcal{Z}(\mathbb{C}(S_n))$ from section 3 it is natural to ask if we can formulate a holographically dual gravitational detection problem for $\mathcal{K}(n)$. This algebra has been studied [30][31] in connection with invariant observables for tensor models. These in turn have been related [69] to the SYK models [70, 71]. A holographic correspondence between SYK and near- AdS_2 quantum gravity has been discussed (see the original papers [72, 73, 74] and a recent review which discusses the correspondence and associated subtleties [75]). It is an interesting question whether near- AdS_2 gravity allows a classical gravity dual of the projector detection in $\mathcal{K}(n)$ analogous to the classical gravity dual of projector detection in $\mathcal{Z}(\mathbb{C}(S_n))$ based on LLM geometries [11] which we described in section 4.

7 Detection of the Littlewood-Richardson projector

Given two non negative integers m and n , there is a PCA $\mathcal{A}(m, n)$ which is relevant for the counting of polynomial functions of two matrices X, Y invariant under adjoint action by unitary matrices $U : (X, Y) \rightarrow (UXU^\dagger, UYU^\dagger)$. We present a review of the background from [30].

$\mathcal{A}(m, n)$ is the subalgebra of $\mathbb{C}(S_{m+n})$ made of the elements that are invariant under the adjoint action of $S_m \times S_n$. There is a basis of $\mathcal{A}(m, n)$ labelled by multi-necklaces with m beads of one colour and n beads of another colour. These are in 1-1 correspondence with orbits in S_{m+n} generated by the conjugation action of $\gamma \in S_m \times S_n \subset S_{m+n}$. With r running over these necklaces,

$$E_r = \sum_{\gamma \in S_m \times S_n} \gamma \sigma^{(r)} \gamma^{-1}, \quad (7.1)$$

where $\sigma^{(r)} \in S_{m+n}$ is a representative of the r 'th orbit. One shows that $\mathcal{A}(m, n)$ is a semi-simple associative algebra and therefore admits a Wedderburn-Artin decomposition. It is proved that

$$\text{Dim}(\mathcal{A}(m, n)) = \sum_{R \vdash m+n, R_1 \vdash m, R_2 \vdash n} g(R_1, R_2, R)^2 \quad (7.2)$$

where $g(R, R_1, R_2)$ is the so-called Littlewood-Richardson (LR) coefficient.

There is a Wedderburn-Artin basis of $\mathcal{A}(m, n)$ in the form $Q_{R_1, R_2; \mu\nu}^R$ with R, R_1, R_2 being Young diagrams with $m+n, m, n$ boxes respectively. The Littlewood-Richardson coefficient determines the range of the indices $\mu, \nu : 1 \leq \mu, \nu \leq g(R_1, R_2, R)$. Explicit formulae for $Q_{R_1, R_2; \mu\nu}^R$ are known in terms of matrix elements of permutations in the irrep R of S_{m+n} along with branching coefficients for the reduction of the irrep R into representations of the subgroup $S_m \times S_n$. The centre $\mathcal{Z}(\mathcal{A}(m, n))$ is spanned by projectors labelled by triples (R_1, R_2, R_3) with non-vanishing $g(R_1, R_2, R)$. They can be written in terms of characters :

$$P_{R_1, R_2}^R = \frac{d_R d_{R_1} d_{R_2}}{(m+n)! m! n!} \sum_{\sigma \in S_{m+n}} \sum_{\sigma_1 \in S_m} \sum_{\sigma_2 \in S_n} \chi_R(\sigma) \chi_{R_1}(\sigma_1) \chi_{R_2}(\sigma_2) \sigma(\sigma_1 \circ \sigma_2) \quad (7.3)$$

TASK: Identify a triple (R, R_1, R_2) for a LR-projector P_{R_1, R_2}^R

We proceed again by making explicit our set of unitaries that will serve in the QPE of this system. For all n , we introduce the notation $T_\mu^{(S_n)}$ which keeps its meaning of (2.1), but use the superscript S_n as we are dealing with different symmetric group in the present formalism. As usual μ will be restricted to $[k, 1^{n-k}]$. We also introduce

$$\chi_{n,k}^{\max} = \max_{R \vdash n} \widehat{\chi}^R(T_k^{(S_n)}) \quad (7.4)$$

and define the unitary operators

$$\begin{aligned}
U_{m,k}^{(1)} &= e^{\frac{2\pi i}{\chi_{m,k}^{\max}} T_k^{(S_m)}} \otimes 1 \\
U_{n,k}^{(2)} &= 1 \otimes e^{\frac{2\pi i}{\chi_{n,k}^{\max}} T_k^{(S_n)}} \\
U_{m+n,k}^{(3)} &= e^{\frac{2\pi i}{\chi_{m+n,k}^{\max}} T_k^{(S_{m+n})}}
\end{aligned} \tag{7.5}$$

These operators satisfy the eigenvalue equations

$$\begin{aligned}
U_{m,k}^{(1)} P_{R_1, R_2}^R &= e^{\frac{2\pi i}{\chi_{n,k}^{\max}} \widehat{\chi}^{R_1}(T_k^{(S_m)})} P_{R_1, R_2}^R, \\
U_{n,k}^{(2)} P_{R_1, R_2}^R &= e^{\frac{2\pi i}{\chi_{n,k}^{\max}} \widehat{\chi}^{R_2}(T_k^{(S_n)})} P_{R_1, R_2}^R, \\
U_{m+n,k}^{(3)} P_{R_1, R_2}^R &= e^{\frac{2\pi i}{\chi_{m+n,k}^{\max}} \widehat{\chi}^R(T_k^{(S_{m+n})})} P_{R_1, R_2}^R
\end{aligned} \tag{7.6}$$

for any k . This will play an important role in the QPE formalism. We need to use the values of

$$\begin{aligned}
k_1 &\in \{2, 3, \dots, k_*(m)\} \\
k_2 &\in \{2, 3, \dots, k_*(n)\} \\
k_3 &\in \{2, 3, \dots, k_*(m+n)\}
\end{aligned} \tag{7.7}$$

to detect the Young diagrams R_1, R_2 and R , respectively.

The problem of detecting LR-projectors is formulated as follows:

“Given the set of unitaries $U_{\ell_i, k_i}^{(i)}, U_{\ell_i, k_i}^{(i)}, \dots, U_{\ell_i, k_i}^{(i)}$, $i = 1, 2, 3$, $\ell_1 = m$, $\ell_2 = n$, $\ell_3 = m + n$, $k_i \in \llbracket 2, k_*(\ell_i) \rrbracket$, and state P_{R_1, R_2}^R with unknown $R_i \vdash n_i$, $i = 1, 2$, $R \vdash m + n$, determine which P_{R_1, R_2}^R we have.”

To obtain the query and gate complexities it suffices to use the same reasoning as previously. The difference in this setting is that they become function of the pair (m, n) . The number of bits required to store the different eigenvalues of the operators are listed below:

$$\begin{aligned}
\text{Bits required to store eigenvalues of } T_{k_1}^{(S_m)} &\sim t_1 \sim k_1 \log m \\
\text{Bits required to store eigenvalues of } T_{k_2}^{(S_n)} &\sim t_2 \sim k_2 \log n \\
\text{Bits required to store eigenvalues of } T_{k_3}^{(S_{m+n})} &\sim t_3 \sim k_3 \log(n + m)
\end{aligned} \tag{7.8}$$

We add up the complexities for the measurements of in each sector and find its estimate:

$$\sum_{k_1=2}^{k_*(m)} k_1 \log(m) \sim k_*(m)^2 \log(m), \quad \sum_{k_2=2}^{k_*(n)} k_2 \log(n) \sim k_*(n)^2 \log(n)$$

$$\sum_{k_3=2}^{k_*(n+m)} k_3 \log(m+n) \sim k_*(m+n)^2 \log(m+n) \quad (7.9)$$

If $k_*(p) < p^\alpha$ holds at large p , we have

$$t \sim (m+n)^{2\alpha} \log(m+n) \quad (7.10)$$

and therefore

Query complexity $\in \mathcal{O}(t) \sim \mathcal{O}((m+n)^{2\alpha} \log(m+n))$.

The gate complexity is estimated in the same way:

Gate complexity $\in \mathcal{O}((m+n)^{3\alpha} (\log(m+n))^2)$.

Acknowledgements

We are pleased to thank Stephon Alexander, George Barnes, Robert de Mello Koch, Humberto Gilmer, Antal Jevicki, Caroline Klivans, Yangrui Hu, Garreth Kemp, David Lowe, Tucker Manton and Adrian Padellaro for insightful discussions during the course of the project. SR is supported by the STFC consolidated grant ST/P000754/1 ‘‘String Theory, Gauge Theory and Duality’’. The authors acknowledge support of the Institut Henri Poincar e (UAR 839 CNRS-Sorbonne Universit e), and LabEx CARMIN (ANR-10-LABX-59-01). SR acknowledges the theoretical physics group at Brown University and the Perimeter Institute for hospitality during the final stages of completion of this work.

A Representation theory lemmas used in quantum-inspired classical algorithms

This appendix provides the proof of two lemmas used in section 5 and further remarks.

Proof of Lemma 1 We start with the definition of the representation matrix element of a projector

$$D_{\gamma\mu}^{\text{reg}}(P_R) = \sum_{\sigma} \frac{d_R \chi_R(\sigma)}{n!} D_{\gamma\mu}^{\text{reg}}(\sigma) = \sum_{\sigma} \frac{d_R \chi_R(\sigma)}{n!} \delta(\gamma^{-1} \sigma \mu) \quad (\text{A.1})$$

Taking the sum of squares, we obtain

$$\begin{aligned} & \sum_{\gamma} (D_{\gamma\mu}^{\text{reg}}(P_R))^2 \\ &= \sum_{\gamma} \frac{1}{(n!)^2} \sum_{\sigma_1} d_R \chi^R(\sigma_1) \delta(\gamma^{-1} \sigma_1 \mu) \sum_{\sigma_2} d_R \chi^R(\sigma_2) \delta(\gamma^{-1} \sigma_2 \mu) \end{aligned}$$

$$\begin{aligned}
&= \sum_{\sigma_1, \sigma_2} d_R^2 \chi^R(\sigma_1) \chi^R(\sigma_2) \delta(\mu^{-1} \sigma_1^{-1} \sigma_2) \mu \\
&= \sum_{\sigma_1, \sigma_2} \frac{d_R^2}{(n!)^2} \chi^R(\sigma_1) \chi^R(\sigma_2) \delta(\sigma_1^{-1} \sigma_2) \\
&= \sum_{\sigma_1} \frac{d_R^2}{(n!)^2} \chi^R(\sigma_1) \chi^R(\sigma_1) \\
&= \frac{d_R^2}{n!}
\end{aligned} \tag{A.2}$$

Remark. This is independent of the choice of μ and is the Plancherel probability weight for the irrep R .

Proof of Lemma 2

$$\begin{aligned}
\sum_{\tau} (D_{\sigma\tau}^{\text{reg}}(T_2))^2 &= \sum_{\tau} \delta(\sigma^{-1} T_2 \tau) \delta(\sigma^{-1} T_2 \tau) \\
&= \delta(\sigma^{-1} T_2^2 \sigma) \\
&= \delta(T_2^2) = \frac{n(n-1)}{2}
\end{aligned} \tag{A.3}$$

B Solving the power sums M_k

The problem of solving the power sum moments $M_k = \sum_{i=1}^N f_i^k$ can be sorted by a simple resolution of a linear system that we now present.

We equate

$$\sum_{f \in \mathcal{F}} A^l(f) = \sum_{k=0}^l c_k^l M_k \tag{B.1}$$

and expand the l.h.s using equation (3.9) in [24]

$$\begin{aligned}
\sum_{f \in \mathcal{F}} A^l(f) &= \sum_{i=1}^N A^l(f_i) = \sum_{i=1}^N l! \sum_{r=0}^l \binom{l}{r} \binom{f_i}{r} 2^r \\
&= \sum_{r=0}^l \frac{2^r l!}{r!} \binom{l}{r} \sum_{i=1}^N (f_i)_r = \sum_{r=0}^l \frac{2^r l!}{r!} \binom{l}{r} \sum_{i=1}^N \sum_{k=0}^r s(r, k) f_i^k
\end{aligned} \tag{B.2}$$

where $(f_i)_r = f_i(f_i - 1) \dots (f_i - r + 1)$ is the falling factorial, and $s(k, r)$'s are Stirling numbers of the first kind. This expands further as

$$\sum_{f \in \mathcal{F}} A^l(f) = \sum_{k=0}^l \left[\sum_{r=k}^l s(r, k) \frac{2^r l!}{r!} \binom{l}{r} \right] \left(\sum_{i=1}^N f_i^k \right) = \sum_{k=0}^l \left[\sum_{r=k}^l s(r, k) \frac{2^r l!}{r!} \binom{l}{r} \right] M_k \tag{B.3}$$

Thus the coefficient c_k is

$$c_k^l = \sum_{r=k}^l s(r, k) \frac{2^r l!}{r!} \binom{l}{r} \quad (\text{B.4})$$

Fixing $l = 0, 1, \dots, \Lambda$, and having sorted $U(l, \rho) = (-1)^l (l+1) \sum_{f \in \mathcal{F}} A^l(f) / \rho^{2l+2}$, we can invert the above triangular system (B.3) starting from $l = 0$.

C Proof of a property of Kronecker projectors

This appendix proves the relation (6.11). Using $\tilde{P}^{R_1, R_2, R_3}$ in (6.8), $Q_{\mu\mu}^{R'_1, R'_2, R'_3}$ in (6.6), and introducing the notation $\kappa_{R'_1 R'_2} = \frac{d_{R'_1} d_{R'_2}}{(n!)^2}$, we have

$$\begin{aligned} \tilde{P}^{R_1, R_2, R_3} Q_{\mu\mu}^{R'_1, R'_2, R'_3} &= \kappa_{R'_1 R'_2} \frac{d_{R_1} d_{R_2} d_{R_3}}{(n!)^3} \sum_{\tau_1, \tau_2, \tau_3} \sum_{\sigma_1, \sigma_2} \chi^{R_1}(\tau_1) \chi^{R_2}(\tau_2) \chi^{R_3}(\tau_3) \\ &\quad \sum_{i_1, i_2, j_1, j_2, k} D_{i_1 j_1}^{R'_1}(\sigma_1) D_{i_2 j_2}^{R'_2}(\sigma_2) C_{i_1, i_2, k}^{R'_1 R'_2; R'_3, \mu} C_{j_1, j_2, k}^{R'_1 R'_2; R'_3, \mu} \tau_3 \tau_1 \sigma_1 \otimes \tau_3 \tau_2 \sigma_2 \\ &= \kappa_{R'_1 R'_2} \sum_{\tau_1, \tau_2, \tau_3} \sum_{\tilde{\sigma}_1, \tilde{\sigma}_2} \frac{d_{R_1} d_{R_2} d_{R_3}}{(n!)^3} \chi^{R_1}(\tau_1) \chi^{R_2}(\tau_2) \chi^{R_3}(\tau_3) \\ &\quad \sum_{i_1, i_2, j_1, j_2, k} D_{i_1 j_1}^{R'_1}(\tau_1^{-1} \tilde{\sigma}_1) D_{i_2 j_2}^{R'_2}(\tau_2^{-1} \tilde{\sigma}_2) C_{i_1, i_2, k}^{R'_1 R'_2; R'_3, \mu} C_{j_1, j_2, k}^{R'_1 R'_2; R'_3, \mu} \tau_3 \tilde{\sigma}_1 \otimes \tau_3 \tilde{\sigma}_2 \\ &= \delta^{R_1 R'_1} \delta^{R_2 R'_2} \kappa_{R_1 R_2} \sum_{\tau_3} \sum_{\tilde{\sigma}_1, \tilde{\sigma}_2} \frac{d_{R_3} \chi^{R_3}(\tau_3)}{n!} \\ &\quad \sum_{i_1, i_2, j_1, j_2, k} D_{i_1 j_1}^{R_1}(\tilde{\sigma}_1) D_{i_2 j_2}^{R_2}(\tilde{\sigma}_2) C_{i_1, i_2, k}^{R_1, R_2; R_3, \mu} C_{j_1, j_2, k}^{R_1, R_2; R_3, \mu} (\tau_3 \tilde{\sigma}_1 \otimes \tau_3 \tilde{\sigma}_2) \\ &= \delta^{R_1 R'_1} \delta^{R_2 R'_2} \kappa_{R_1 R_2} \sum_{\tau_3} \sum_{\sigma_1, \sigma_2} \frac{d_{R_3} \chi^{R_3}(\tau_3)}{n!} \\ &\quad \sum_{i_1, i_2, j_1, j_2, k} D_{i_1 j_1}^{R_1}(\tau_3^{-1} \sigma_1) D_{i_2 j_2}^{R_2}(\tau_3^{-1} \sigma_2) C_{i_1 i_2 k}^{R_1 R_2 R_3; \mu} C_{j_1 j_2 k}^{R_1 R_2 R_3; \mu} \sigma_1 \otimes \sigma_2 \\ &= \delta^{R_1 R'_1} \delta^{R_2 R'_2} \kappa_{R_1 R_2} \sum_{\sigma_1, \sigma_2} \sum_{i_1, i_2, j_1, j_2} D_{i_1 p_1}^{R_1}(\tau_3^{-1}) D_{p_1 j_1}^{R_1}(\sigma_1) D_{i_2 p_2}^{R_2}(\tau_3^{-1}) D_{p_2 j_2}^{R_2}(\sigma_2) \\ &\quad \times C_{i_1 i_2 k}^{R_1, R_2, R_3; \mu} C_{j_1 j_2 k}^{R_1, R_2, R_3; \mu} \sigma_1 \otimes \sigma_2 \\ &= \delta^{R_1 R'_1} \delta^{R_2 R'_2} \delta^{R_3 R'_3} \kappa_{R_1 R_2} \sum_{\sigma_1, \sigma_2} D_{p_1 j_1}^{R_1}(\sigma_1) D_{p_2 j_2}^{R_2}(\sigma_2) \\ &\quad \times C_{p_1, p_2, k'}^{R_1, R_2, R_3} D_{k' k}^{R'_3}(\tau_3) \delta^{\nu\mu} \frac{d_{R_3} \chi^{R_3}(\tau_3)}{n!} C_{j_1, j_2, k}^{R_1 R_2; R_3, \mu} \sigma_1 \otimes \sigma_2 \\ &= \delta^{R_1 R'_1} \delta^{R_2 R'_2} \delta^{R_3 R'_3} \kappa_{R_1 R_2} \sum_{\sigma_1, \sigma_2} D_{p_1 j_1}^{R_1}(\sigma_1) D_{p_2 j_2}^{R_2}(\sigma_2) C_{p_1, p_2, k}^{R_1, R_2; R_3, \mu} C_{j_1, j_2, k}^{R_1, R_2; R_3, \mu} \sigma_1 \otimes \sigma_2 \\ &= \delta^{R_1, R'_1} \delta^{R_2, R'_2} \delta^{R_3, R'_3} Q_{\mu\mu}^{R_1, R_2, R_3} \end{aligned} \quad (\text{C.1})$$

References

- [1] Juan Martin Maldacena. The Large N limit of superconformal field theories and supergravity. *Adv. Theor. Math. Phys.*, 2:231–252, 1998.
- [2] S. S. Gubser, Igor R. Klebanov, and Alexander M. Polyakov. Gauge theory correlators from noncritical string theory. *Phys. Lett. B*, 428:105–114, 1998.
- [3] Edward Witten. Anti-de Sitter space and holography. *Adv. Theor. Math. Phys.*, 2:253–291, 1998.
- [4] David J. Gross and Washington Taylor. Two-dimensional QCD is a string theory. *Nucl. Phys. B*, 400:181–208, 1993.
- [5] Stefan Cordes, Gregory W. Moore, and Sanjaye Ramgoolam. Lectures on 2-d Yang-Mills theory, equivariant cohomology and topological field theories. *Nucl. Phys. B Proc. Suppl.*, 41:184–244, 1995.
- [6] Arun Ram. *Dissertation, Chapter 1: Representation theory*. 2004.
- [7] Nielsen, Michael A. and Chuang, Isaac L. *Quantum Computation and Quantum Information: 10th Anniversary Edition*. Cambridge University Press, 2010.
- [8] Sangmin Lee, Shiraz Minwalla, Mukund Rangamani, and Nathan Seiberg. Three point functions of chiral operators in $D = 4$, $N=4$ SYM at large N. *Adv. Theor. Math. Phys.*, 2:697–718, 1998.
- [9] Ofer Aharony, Steven S. Gubser, Juan Martin Maldacena, Hiroshi Ooguri, and Yaron Oz. Large N field theories, string theory and gravity. *Phys. Rept.*, 323:183–386, 2000.
- [10] John McGreevy, Leonard Susskind, and Nicolaos Toumbas. Invasion of the giant gravitons from Anti-de Sitter space. *JHEP*, 06:008, 2000.
- [11] Hai Lin, Oleg Lunin, and Juan Martin Maldacena. Bubbling AdS space and 1/2 BPS geometries. *JHEP*, 10:025, 2004.
- [12] Steve Corley, Antal Jevicki, and Sanjaye Ramgoolam. Exact correlators of giant gravitons from dual $N=4$ SYM theory. *Adv. Theor. Math. Phys.*, 5:809–839, 2002.
- [13] Steven Corley and Sanjaye Ramgoolam. Finite factorization equations and sum rules for BPS correlators in $N=4$ SYM theory. *Nucl. Phys. B*, 641:131–187, 2002.
- [14] A. Bissi, C. Kristjansen, D. Young, and K. Zoubos. Holographic three-point functions of giant gravitons. *JHEP*, 06:085, 2011.

- [15] Pawel Caputa, Robert de Mello Koch, and Konstantinos Zoubos. Extremal versus Non-Extremal Correlators with Giant Gravitons. *JHEP*, 08:143, 2012.
- [16] Hai Lin. Giant gravitons and correlators. *JHEP*, 12:011, 2012.
- [17] Charlotte Kristjansen, Stefano Mori, and Donovan Young. On the Regularization of Extremal Three-point Functions Involving Giant Gravitons. *Phys. Lett. B*, 750:379–383, 2015.
- [18] Yunfeng Jiang, Shota Komatsu, and Edoardo Vescovi. Structure constants in $\mathcal{N} = 4$ SYM at finite coupling as worldsheet g-function. *JHEP*, 07(07):037, 2020.
- [19] Peihe Yang, Yunfeng Jiang, Shota Komatsu, and Jun-Bao Wu. D-branes and orbit average. *SciPost Phys.*, 12(2):055, 2022.
- [20] Gaoli Chen, Robert de Mello Koch, Minkyoo Kim, and Hendrik J. R. Van Zyl. Absorption of closed strings by giant gravitons. *JHEP*, 10:133, 2019.
- [21] Adolfo Holguin and Wayne W. Weng. Orbit Averaging Coherent States: Holographic Three-Point Functions of AdS Giant Gravitons. 11 2022.
- [22] Robert de Mello Koch, Jia-Hui Huang, Minkyoo Kim, and Hendrik J. R. Van Zyl. Emergent Yang-Mills theory. *JHEP*, 10:100, 2020.
- [23] Sanjaye Ramgoolam and Lewis Sword. Matrix and tensor witnesses of hidden symmetry algebras. *JHEP*, 03:056, 2023.
- [24] Vijay Balasubramanian, Bartłomiej Czech, Klaus Larjo, and Joan Simon. Integrability versus information loss: A Simple example. *JHEP*, 11:001, 2006.
- [25] Garreth Kemp and Sanjaye Ramgoolam. BPS states, conserved charges and centres of symmetric group algebras. *JHEP*, 01:146, 2020.
- [26] Leonard Susskind. Computational Complexity and Black Hole Horizons. *Fortsch. Phys.*, 64:24–43, 2016. [Addendum: Fortsch.Phys. 64, 44–48 (2016)].
- [27] Adam Bouland, Bill Fefferman, and Umesh Vazirani. Computational pseudorandomness, the wormhole growth paradox, and constraints on the AdS/CFT duality. 10 2019.
- [28] Iosif Bena, Emil J. Martinec, Samir D. Mathur, and Nicholas P. Warner. Fuzzballs and Microstate Geometries: Black-Hole Structure in String Theory. 4 2022.
- [29] Ewin Tang. A quantum-inspired classical algorithm for recommendation systems. In *Proceedings of the 51st Annual ACM SIGACT Symposium on Theory of Computing, STOC 2019*, page 217–228, New York, NY, USA, 2019. Association for Computing Machinery.

- [30] Paolo Mattioli and Sanjaye Ramgoolam. Permutation Centralizer Algebras and Multi-Matrix Invariants. *Phys. Rev. D*, 93(6):065040, 2016.
- [31] Joseph Ben Geloun and Sanjaye Ramgoolam. Tensor Models, Kronecker coefficients and Permutation Centralizer Algebras. *JHEP*, 11:092, 2017.
- [32] Joseph Ben Geloun and Sanjaye Ramgoolam. Quantum mechanics of bipartite ribbon graphs: Integrality, Lattices and Kronecker coefficients. *Algebraic Combinatorics, to appear*, 10 2020.
- [33] Yusuke Kimura and Sanjaye Ramgoolam. Branes, anti-branes and Brauer algebras in gauge-gravity duality. *JHEP*, 11:078, 2007.
- [34] Thomas William Brown, P. J. Heslop, and S. Ramgoolam. Diagonal multi-matrix correlators and BPS operators in N=4 SYM. *JHEP*, 02:030, 2008.
- [35] Rajsekhar Bhattacharyya, Storm Collins, and Robert de Mello Koch. Exact Multi-Matrix Correlators. *JHEP*, 03:044, 2008.
- [36] Rajsekhar Bhattacharyya, Robert de Mello Koch, and Michael Stephanou. Exact Multi-Restricted Schur Polynomial Correlators. *JHEP*, 06:101, 2008.
- [37] Yusuke Kimura and Sanjaye Ramgoolam. Enhanced symmetries of gauge theory and resolving the spectrum of local operators. *Phys. Rev. D*, 78:126003, 2008.
- [38] Jurgis Pasukonis and Sanjaye Ramgoolam. Quivers as Calculators: Counting, Correlators and Riemann Surfaces. *JHEP*, 04:094, 2013.
- [39] Yusuke Kimura. Multi-matrix models and Noncommutative Frobenius algebras obtained from symmetric groups and Brauer algebras. *Commun. Math. Phys.*, 337(1):1–40, 2015.
- [40] Sergey Bravyi, Anirban Narayan Chowdhury, David Gosset, Vojtech Havlicek, and Guanyu Zhu. Quantum complexity of the kronecker coefficients. *ArXiv*, abs/2302.11454, 2023.
- [41] Morton Hamermesh. *Group theory and its application to Physical Problems*. Dover Books on Physics. Dover, 2003.
- [42] Sanjaye Ramgoolam and Eric Sharpe. Combinatoric topological string theories and group theory algorithms. *JHEP*, 10:147, 2022.
- [43] Michel Lassalle. An explicit formula for the characters of the symmetric group. *Mathematische Annalen*, 340:383–405, 2007.

- [44] Sylvie Corteel, Alain Goupil, and Gilles Schaeffer. Content evaluation and class symmetric functions. *Advances in Mathematics*, 188:315–336, 2004.
- [45] O. Ganor, J. Sonnenschein, and S. Yankielowicz. The String theory approach to generalized 2-D Yang-Mills theory. *Nucl. Phys. B*, 434:139–178, 1995.
- [46] Troels Harmark and Marta Orselli. Spin Matrix Theory: A quantum mechanical model of the AdS/CFT correspondence. *JHEP*, 11:134, 2014.
- [47] M. Lasalle. An explicit formula for the characters of the symmetric group. *Mathematische Annalen*, 340:383–405.
- [48] Valentin Féray and Piotr Śniady. Asymptotics of characters of symmetric groups related to stanley character formula. *Annals of Mathematics*, 173(2):887–906, mar 2011.
- [49] Barry Simon. *Representations of finite and compact groups*. American Mathematical Society, 1991.
- [50] David Berenstein. A Toy model for the AdS / CFT correspondence. *JHEP*, 07:018, 2004.
- [51] Yastoshi Takayama and Asato Tsuchiya. Complex matrix model and fermion phase space for bubbling AdS geometries. *JHEP*, 10:004, 2005.
- [52] Vijay Balasubramanian, Jan de Boer, Vishnu Jejjala, and Joan Simon. The Library of Babel: On the origin of gravitational thermodynamics. *JHEP*, 12:006, 2005.
- [53] Ming-Po Chen and H.M. Srivastava. Orthogonality relations and generating functions for Jacobi polynomials and related hypergeometric functions. *Applied Mathematics and Computation*, 68(2):153–188, 1995.
- [54] Paul S. Heckbert. Fourier Transforms and the Fast Fourier Transform (FFT) Algorithm. *Note 2, Computer Graphics 2*, pages 15–463, 1998.
- [55] David Harvey and Joris van der Hoeven. Integer multiplication in time $O(n \log n)$. *Annals of Mathematics*, 193(2):563 – 617, 2021.
- [56] Qiaochu Yuan (<https://mathoverflow.net/users/290/qiaochu-yuan>). What determines the maximal dimension of the irreps of a (finite) group? MathOverflow. URL:<https://mathoverflow.net/q/373786> (version: 2020-10-10).
- [57] Aram W. Harrow, Avinatan Hassidim, and Seth Lloyd. Quantum algorithm for linear systems of equations. *Phys. Rev. Lett.*, 103:150502, Oct 2009.

- [58] Scott Aaronson. Quantum Machine Learning algorithms: read the fine print. *Nature Physics*, 11:291–293, 2015.
- [59] user2345678 (<https://math.stackexchange.com/users/314957/user2345678>). $s_n, n \geq 1$ has precisely two 1-dimensional irreducible representations. Mathematics Stack Exchange. URL:<https://math.stackexchange.com/q/2784937> (version: 2018-05-17).
- [60] zibadawa timmy (<https://math.stackexchange.com/users/92067/zibadawa-timmy>). One-dimensional representations of s_5 . Mathematics Stack Exchange. URL:<https://math.stackexchange.com/q/898008> (version: 2014-08-15).
- [61] (<https://math.stackexchange.com/users/280033/e.g>). Show the commutator subgroup of s_n is a_n for $n \geq 5$. Mathematics Stack Exchange. URL:<https://math.stackexchange.com/q/1505560> (version: 2015-10-30).
- [62] Joseph Ben Geloun and Sanjaye Ramgoolam. Counting tensor model observables and branched covers of the 2-sphere. *Ann. Inst. H. Poincaré D Comb. Phys. Interact.*, 1(1):77–138, 2014.
- [63] Joseph Ben Geloun. On the counting tensor model observables as $U(N)$ and $O(N)$ classical invariants. *PoS, CORFU2019*:175, 2020.
- [64] Joseph Ben Geloun and Sanjaye Ramgoolam. All-orders asymptotics of tensor model observables from symmetries of restricted partitions. *J. Phys. A*, 55(43):435203, 2022.
- [65] Ketan Mulmuley and Milind A. Sohoni. Geometric complexity theory i: An approach to the p vs. np and related problems. *SIAM J. Comput.*, 31:496–526, 2001.
- [66] Peter Burgisser, Matthias Christandl, and Christian Ikenmeyer. Nonvanishing of kronecker coefficients for rectangular shapes. *Advances in Mathematics*, 227:2082–2091, 2011.
- [67] Christian Ikenmeyer, Ketan Mulmuley, and Michael Walter. On vanishing of kronecker coefficients. *Computational Complexity*, 26:949–992, 2017.
- [68] Igor Pak, Greta Panova, and Damir Yeliussizov. On the largest kronecker and littlewood-richardson coefficients. *Journal of Combinatorial Theory, Series A*, 165:44–77, 2019.
- [69] Edward Witten. An SYK-Like Model Without Disorder. *J. Phys. A*, 52(47):474002, 2019.
- [70] Subir Sachdev and Jinwu Ye. Gapless spin-fluid ground state in a random quantum heisenberg magnet. *Phys. Rev. Lett.*, 70:3339–3342, May 1993.

- [71] Alexei Kitaev. A simple model of quantum holography. Caltech and KITP workshop 2015.
- [72] Joseph Polchinski and Vladimir Rosenhaus. The Spectrum in the Sachdev-Ye-Kitaev Model. *JHEP*, 04:001, 2016.
- [73] Antal Jevicki, Kenta Suzuki, and Junggi Yoon. Bi-Local Holography in the SYK Model. *JHEP*, 07:007, 2016.
- [74] Juan Maldacena, Douglas Stanford, and Zhenbin Yang. Conformal symmetry and its breaking in two dimensional Nearly Anti-de-Sitter space. *PTEP*, 2016(12):12C104, 2016.
- [75] Gábor Sárosi. AdS₂ holography and the SYK model. *PoS*, Modave2017:001, 2018.